The Cranial Anatomy of the Long-Snouted Tyrannosaurid Dinosaur Qianzhousaurus sinensis from the Upper Cretaceous of China

Authors: Foster, William, Brusatte, Stephen L., Carr, Thomas D., Williamson, Thomas E., Yi, Laiping, et al.

Source: Journal of Vertebrate Paleontology, 41(4)

Published By: The Society of Vertebrate Paleontology

URL: https://doi.org/10.1080/02724634.2021.1999251

Journal of Vertebrate Paleontology e1999251 (30 pages)
Published with license by the Society of Vertebrate Paleontology
DOI: 10.1080/02724634.2021.1999251

ARTICLE

THE CRANIAL ANATOMY OF THE LONG-SNOUTED TYRANNOSAURID DINOSAUR *QIANZHOUSAURUS SINENSIS* FROM THE UPPER CRETACEOUS OF CHINA

WILLIAM FOSTER, [1*] STEPHEN L. BRUSATTE, [1*] THOMAS D. CARR, [2] THOMAS E. WILLIAMSON, [3] LAIPING YI,[4] and JUNCHANG LÜ†[5]
[1]School of Geosciences, University of Edinburgh, Grant Institute, James Hutton Road, Edinburgh EH9 3FE, U.K., william.foster.eng@gmail.com, Stephen.Brusatte@ed.ac.uk;
[2]Department of Biology, Carthage College, 2001 Alford Park Drive, Kenosha, WI 53140, U.S.A., tcarr@carthage.edu;
[3]New Mexico Museum of Natural History and Science, Albuquerque, New Mexico, 87104, U.S.A., Thomas.Williamson@state.nm.us;
[4]Ganzhou Museum, Ganzhou 341000, Jiangxi Province, China;
[5]Institute of Geology, Chinese Academy of, Geological Sciences, Beijing, China

ABSTRACT—Tyrannosaurid theropods topped the terrestrial food chain in North America and Asia during the latest Cretaceous. Most tyrannosaurids, exemplified by *Tyrannosaurus rex*, had deep snouts, thick teeth, and large jaw muscles that could generate high bite forces. They coexisted in Asia with a morphologically divergent group of long-snouted relatives, called alioramins. *Qianzhousaurus sinensis*, from the Maastrichtian of Ganzhou, China, is the largest alioramin yet discovered, but has only been briefly described. Here we present a detailed osteological description of the holotype cranium and mandible of *Qianzhousaurus*. We identify several new autapomorphic features of the genus, and new synapomorphies that unite alioramins (*Qianzhousaurus*, *Alioramus altai*, *Alioramus remotus*) as a clade, including a laterally projecting rugosity on the jugal. We clarify that the elongate skull of alioramins involves lengthening of the anterior palate but not the premaxilla, and is reflected by lengthening of the posterior bones of the lower jaw, even though the posterior cranium (orbit and lateral temporal fenestra) are proportionally similar to deep-skulled tyrannosaurids. We show that much of the variation among the alioramin species is consistent with growth trends in other tyrannosaurids, and that *A. altai*, *A. remotus*, and *Qianzhousaurus* represent different ontogenetic stages of progressive maturity, across which the signature nasal rugosites of alioramins became less prominent. We predict that the holotype skull of *Qianzhousaurus* represents the adult level of maturity for alioramins, and propose that the skull morphology of *Qianzhousaurus* indicates a much weaker bite than deep-skulled tyrannosaurids, suggestive of differences in prey choice and feeding style.

SUPPLEMENTAL DATA—Supplemental materials are available for this article for free at www.tandfonline.com/UJVP.

Citation for this article: Foster, W., S. L. Brusatte, T. D. Carr, T. E. Williamson, L. Yi, and J. Lü. 2022. The cranial anatomy of the long-snouted tyrannosaurid dinosaur *Qianzhousaurus sinensis* from the Upper Cretaceous of China. Journal of Vertebrate Paleontology. DOI: 10.1080/02724634.2021.1999251

INTRODUCTION

The naming and comparative description of the Late Cretaceous Chinese theropod dinosaur *Qianzhousaurus sinensis* by Lü et al. (2014) solidified the hypothesis of a clade of long-snouted species, called Alioramini, within derived Tyrannosauridae, the classic group of colossal Late Cretaceous super-predators that dominated their ecosystems in the latest stages of the Mesozoic. The three currently known members of Alioramini—*Alioramus remotus* (Kurzanov, 1976), *Alioramus altai* (Brusatte et al., 2009, 2012; Bever et al., 2011, 2013), and *Qianzhousaurus sinensis*—are now recognized as being divergent in skeletal morphology to other derived tyrannosaurids, most notably in their longirostrine skulls and more extensive ornamentation on the dorsal snout surface than in most tyrannosaurid taxa.

Research documenting longirostrine tyrannosaurids began in the mid-late 20th century when the first of the alioramins, *Alioramus remotus*, was uncovered in Mongolia at the Nogon Tsav locality, Bayankhnongor Aimag (likely Maastrichtian) (Kurzanov, 1976). Now housed in the Paleontological Institute in Moscow (PIN 3141/1), the specimen consists of disarticulated cranial and limited postcranial material. Despite being largely fragmentary, the find included enough evidence for Kurzanov (1976) to identify it as tyrannosaurid and to establish it as a new genus. Kurzanov (1976) also noted considerable morphological deviation between the longirostrine *Alioramus* and other derived tyrannosaurids such as *Tyrannosaurus* and *Tarbosaurus*, which exhibit the classic tyrannosaurid characteristics: wide and deep skulls alongside heavy-set bodies.

The holotype of *Alioramus altai* (IGM 100/1844), also from Mongolia (Nemegt Formation, Maastrichtian), is substantially more complete than that of *A. remotus*, consisting of a nearly complete and superbly preserved skull from a juvenile-to-subadult individual (Brusatte et al., 2009). As is the case in

*Corresponding author.
†Deceased
This article has been corrected with minor changes. These changes do not impact the academic content of the article.

Color versions of one or more of the figures in the article can be found online at www.tandfonline.com/ujvp.

A. remotus, the skull morphology is highly gracile and elongate, and different from the deeper skulls of juveniles of the large tyrannosaurid *Tarbosaurus*, indicating that these *Alioramus* individuals are not juveniles of larger deep-snouted tyrannosaurid taxa. Phylogenetic analysis of the skeleton placed *A. altai* as closely related to the large derived tyrannosaurids such as *Tyrannosaurus* and *Tarbosaurus* (Brusatte et al., 2009, 2010). The well-preserved *A. altai* specimen was later monographed by Brusatte et al. (2012), who provided further arguments that *Alioramus* was morphologically and proportionally distinct from similarly sized *Tarbosaurus* individuals. In sum, this work concluded: (1) that the genus *Alioramus* is valid and does not simply consist of juvenile *Tarbosaurus* specimens, (2) that there are enough significant differences between *A. remotus* and *A. altai* to distinguish the latter as a new taxon within the *Alioramus* genus, and (3) that the significantly divergent body plan of both *Alioramus* taxa from that of the large derived tyrannosaurids suggests significant differences in ecology and behavior.

In 2014, another specimen of a long-snouted tyrannosaurid from the Upper Cretaceous of Asia was uncovered from the the Nanxiong Formation (Maastrichtian) on a construction site in Longling Town, within Jiangxi Province of Southeast China: a well-preserved skeleton with a nearly complete skull, which was described as the holotype of *Qianzhousaurus sinensis* (GM F10004). The short, initial description of the specimen by Lü et al. (2014) provided further evidence that the long-snouted tyrannosaurids are a unique lineage, not juveniles of deep-skulled taxa. As is the case for both members of the *Alioramus* genus, the *Q. sinensis* holotype possesses a long, gracile skull and prominent cranial ornamentation. Importantly, the specimen is considerably larger and more mature than the holotypes of the two *Alioramus* species, exhibiting many features that occur late in tyrannosaurid ontogeny such as highly fused cranial bones, larger and more developed cranial ornamentation, and a lower number of teeth, which are more robust than in juveniles (incrassate) (Carr, 1999). Lü et al. (2014) presented a phylogenetic analysis that found all three long-snouted species—*Alioramus remotus*, *Alioramus altai*, and *Qianzhousaurus sinensis*—in their own subclade of long-snouted tyrannosaurids, which was named Alioramini. This genealogical arrangement was later corroborated by the tyrannosauroid phylogenetic analyses of Brusatte and Carr (2016) and Carr et al. (2017). (Although see Loewen et al. 2013 for an alternative phylogenetic placement.)

Thus far, the only description of the *Qianzhousaurus sinensis* holotype specimen (GM F10004) is the short initial paper of Lü et al. (2014), which included only three figures of the material. We here present a more thorough description of the cranial anatomy of the specimen (minus the braincase, which will be the subject of a future stand-alone study), in a similar vein to the *Alioramus altai* monograph of Brusatte et al. (2012). In describing the osteology of *Qianzhousaurus*, we make comparisons to its close *Alioramus* relatives and to other tyrannosauroids. Our description adds to the detailed descriptive literature on tyrannosauroid cranial anatomy, which includes important comprehensive descriptions of tyrannosaurids such as *Tyrannosaurus rex* (Osborn, 1912; Molnar, 1991; Brochu, 2003; Carr and Williamson, 2004; Carr, 2020), *Tarbosaurus bataar* (Maleev, 1974; Hurum and Sabbath, 2003), and albertosaurines (Lambe, 1917; Parks, 1928; Russell, 1970; Carr, 1999; Currie, 2003), along with more basal tyrannosauroids such as *Proceratosaurus* (Rauhut et al., 2010), *Dryptosaurus* (Brusatte et al., 2011), and *Appalachiosaurus* (Carr et al., 2005). As *Alioramus altai* has been exhaustively monographed by Brusatte et al. (2012), and is overall very similar in morphology to *Qianzhousaurus*, we do not provide a similar level of verbal description here, but instead describe the most salient features and rely on figures to document the anatomy in detail.

Institutional Abbreviations—CMN, Canadian Museum of Nature, Ottawa, Canada; **GM**, Ganzhou Museum, Ganzhou, China; **IGM**, Institute of Geology, Ulaan Baatar, Mongolia; **PIN**, Paleontological Institute, Moscow, Russia; **ROM**, Royal Ontario Museum, Toronto, Canada.

SYSTEMATIC PALEONTOLOGY

DINOSAURIA Owen, 1842
THEROPODA Marsh, 1881
TETANURAE Gauthier, 1986
COELUROSAURIA von Huene, 1914
TYRANNOSAUROIDEA Osborn, 1905
TYRANNOSAURIDAE Osborn, 1905
TYRANNOSAURINAE Osborn, 1905
ALIORAMINI Olshevsky, 1995 sensu Lü et al., 2014
QIANZHOUSAURUS SINENSIS (Lü et al., 2014)
(Figs. 1–14).

Qianzhousaurus sinensis Lü et al., 2014:figs. 1–3 (original description).

Holotype—Nearly complete skull and almost complete left mandible (GM F10004-1), described in detail herein, along with associated postcranial skeleton (GM F10004-2-8).

Locality and Horizon—Nanxiong Formation (Upper Cretaceous, Maastrichtian), Longling Town, Nakang, Ganzhou City, Jiangxi Province, China.

Updated Diagnosis—Long-snouted tyrannosaurid tyrannosauroid dinosaur with following autapomorphies of the skull: large fenestra on the ascending ramus of the maxilla; extremely reduced premaxilla; laterally straight, rod-like nasal element that does not expand laterally around the naris region; anteroventrally oriented ventral process of lacrimal; gracile and shallow dorsal prong of anterior ramus of squamosal; anteroposteriorly oriented ventral process of squamosal; anterior edge of dentary smoothly merges with ventral dentary margin; highly concave dorsal margin of supradentary. Potential but problematic autapomorphies (see text): an ovoid foramen on the medial surface of prearticular; limited medial exposure of the coronoid in medial view. See Lü et al. (2014) for one additional diagnostic character of the postcranium (absence of pronounced vertical ridge on lateral surface of illium).

Description

Premaxilla—The premaxilla is not preserved in the *Alioramus remotus* and *Alioramus altai* holotypes, making *Qianzhousaurus* the first (and thus only) alioramin for which this bone can be described (Figs. 1, 2). The premaxilla is preserved on both sides of the skull, and is a small bone compared with the rest of the skull, as in tyrannosauroids generally (Brusatte et al., 2014:character 826). It is remarkably small in *Qianzhousaurus*, however, measuring only 2.2% of the overall basal skull length, compared with ~4–10% in other tyrannosauroids (Lü et al., 2014). Thus, despite the longirostrine snout of *Qianzhousaurus*, the premaxilla is not elongated, like the maxilla and nasals are (it is largely the increased length of these bones that make the premaxilla so proportionally small compared with other tyrannosauroids).

The dorsal process of the premaxilla (Fig. 2) contacts the anterior end of the nasal, dorsal to the external naris, permitting both bones to form the dorsal rim of the naris. Contact with the maxilla is via a small, tapering process that contacts or nearly contacts the nasal underneath the floor of the naris (see below) (Fig. 2).

The external naris has the characteristic 'tear-drop' morphology as in most tyrannosaurids (Fig. 2), although the elongate condition of the dorsal ramus of the premaxilla extends further posteriorly along the naris rim than in *Tyrannosaurus* (Brochu, 2003), *Tarbosaurus* (Maleev, 1974), and *Gorgosaurus* (Lambe, 1917). The elongate condition of the dorsal and ventral processes

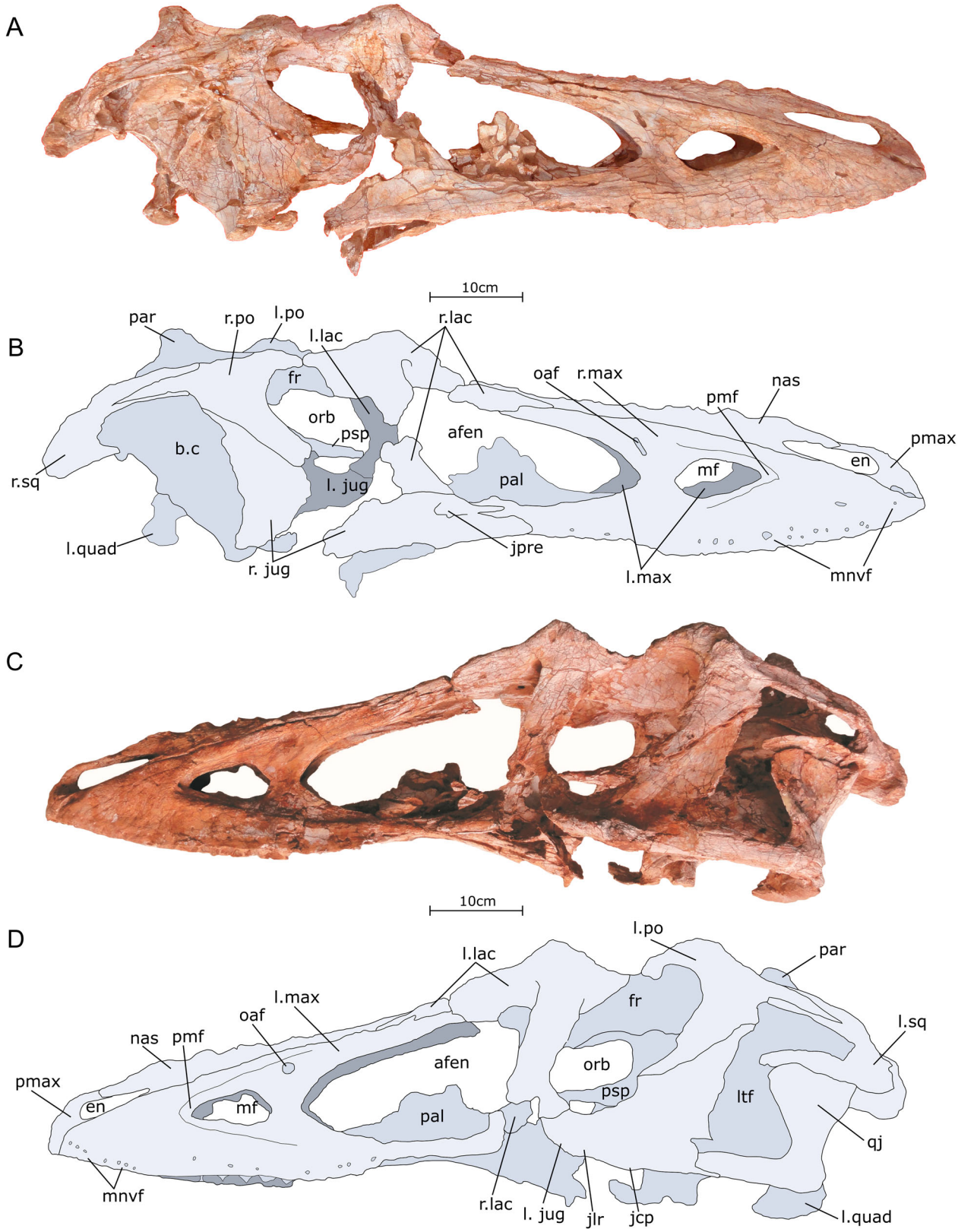

FIGURE 1. Skull of the holotype specimen of *Qianzhousaurus sinensis* (GM F10004). **A**, photograph of skull in right lateral view; **B**, line drawing of skull in right lateral view; **C**, photograph of skull in left lateral view; **D**, line drawing of skull in left lateral view. **Abbreviations**: **afen**, antorbital fenestra; **b.c**, braincase; **en**, external naris; **fr**, frontals; **jcp**, jugal cornual process; **jlr**, jugal lateral rugosities; **jpre**, jugal pneumatic recess; **l. jug**, left jugal; **l. lac**, left lacrimal; **l. max**, left maxilla; **l. po**, left postorbital; **l. quad**, left quadrate; **l. sq**, left squamosal; **ltf**, lateral temporal fenestra; **mf**, maxillary fenestra; **mnvf**, maxillary neurovascular foramina; **nas**, nasal; **oaf**, ovoid accessory foramen; **orb**, orbit; **pal**, palatine; **par**, parietal; **pmax**, premaxilla; **pmf**, premaxillary fossa; **psp**, parasphenoid rostrum; **qj**, quadratojugal; **r. jug**, right jugal; **r. lac**, right lacrimal; **r. max**, right maxilla; **r. po**, right postorbital; **r. sq**, right squamosal.

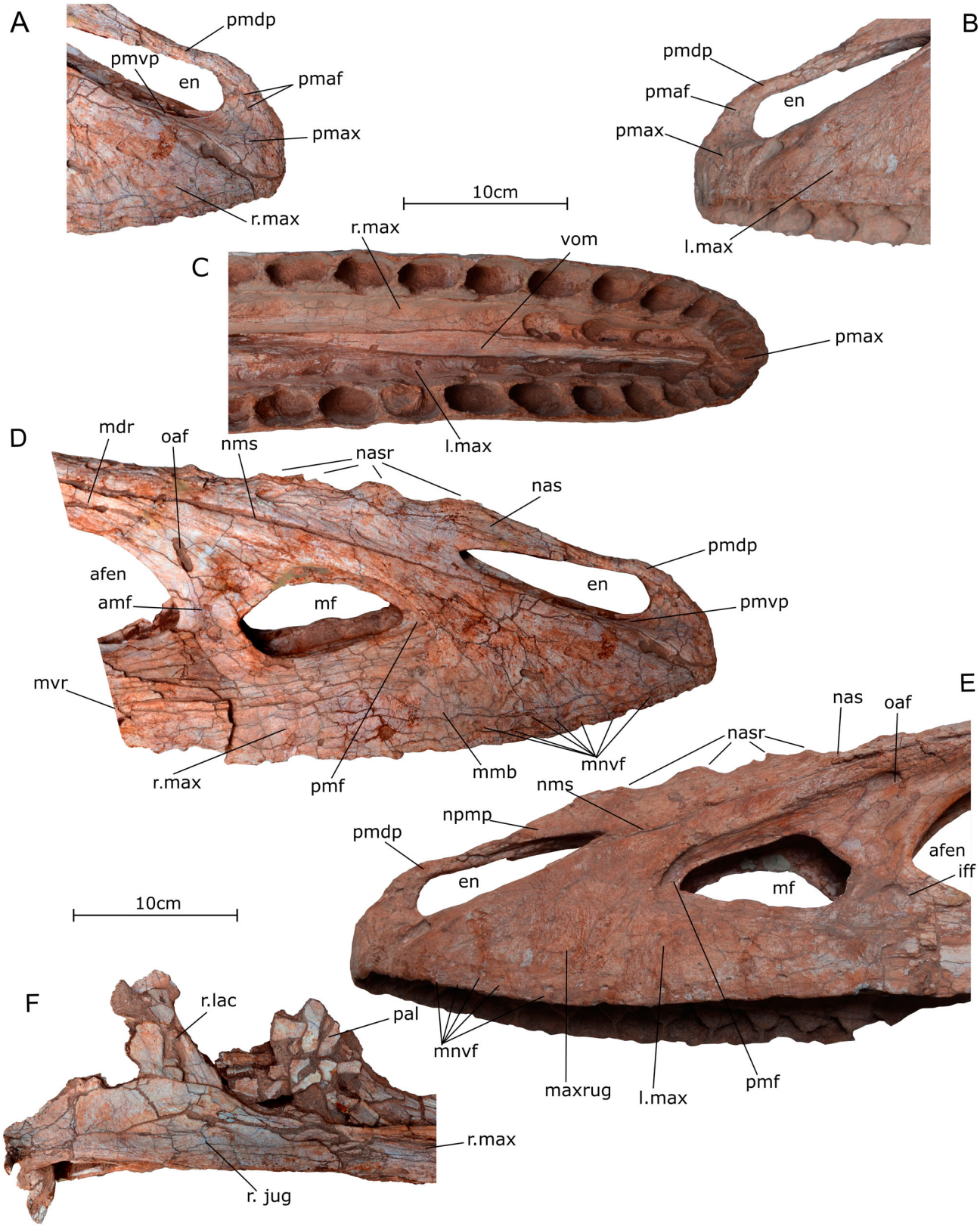

FIGURE 2. Close-ups of the anterior cranium of the holotype specimen of *Qianzhousaurus sinensis* (GM F10004). **A**, premaxilla in right lateral view; **B**, premaxilla in left lateral view; **C**, anterior snout in ventral view; **D**, anterior snout in right lateral view; **E**, anterior snout in left lateral view; **F**, right jugal/lacrimal articular region in right lateral view. **Abbreviations**: **afen**, antorbital fenestra; **amf**, additional maxillary fossa; **en**, external naris; **iff**, intra fenestra foramina; **l. max**, left maxilla; **maxrug**, maxilla rugosity; **mdr**, maxilla dorsal ramus; **mf**, maxillary fenestra; **mmb**, maxillary main body; **mnvf**, maxillary neurovascular foramina; **mvr**, maxillary ventral ramus; **nas**, nasal; **nasr**, nasal rugosities; **nms**, nasal/maxilla suture; **npmp**, nasal premaxillary process; **oaf**, ovoid accessory foramen; **pal**, palatine; **pmaf**, premaxillary accessory foramen; **pmax**, premaxilla; **pmdp**, premaxillary dorsal process; **pmf**, promaxillary fossa; **pmvp**, premaxillary ventral process; **r.jug**, right jugal; **r.lac**, right lacrimal; **r. max**, right maxilla; **vom**, vomer.

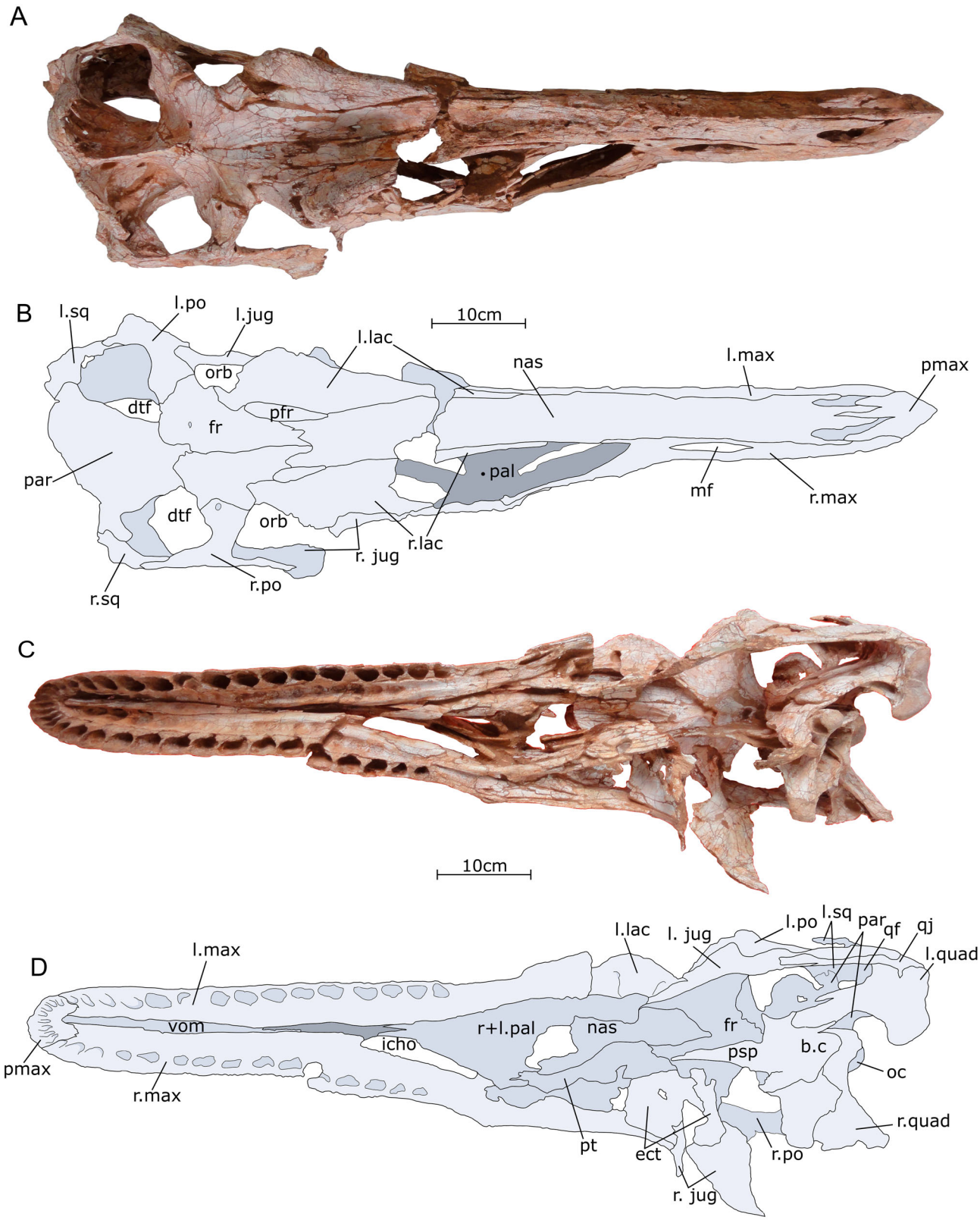

FIGURE 3. Skull of the holotype specimen of *Qianzhousaurus sinensis* (GM F10004). **A**, photograph of skull in dorsal view; **B**, line drawing of skull in dorsal view; **C**, photograph of skull in ventral view; **D**, line drawing of the skull in ventral view. **Abbreviations**: **b.c**, braincase; **dtf**, dorsotemporal fenestra; **ect**, ectopterygoid; **fr**, frontals; **icho**, internal choana; **l. lac**, left lacrimal; **l. max**, left maxilla; **l. po**, left postorbital; **l. quad**, left quadrate; **l. sp**, left squamosal; **mf**, maxillary fenestra; **nas**, nasal; **oc**, occipital condyle; **orb**, orbit; **pal**, palatine; **par**, parietal; **pfr**, prefrontals; **pmax**, premaxilla; **psp**, parasphenoid rostrum; **pt**, pterygoid; **qf**, quadrate foramen; **qj**, quadratojugal; **r. jug**, right jugal; **r. lac**, right lacrimal; **r. max**, right maxilla; **r. po**, right postorbital; **r. quad**, right quadrate; **r. sq**, right squamosal; **vom**, vomer.

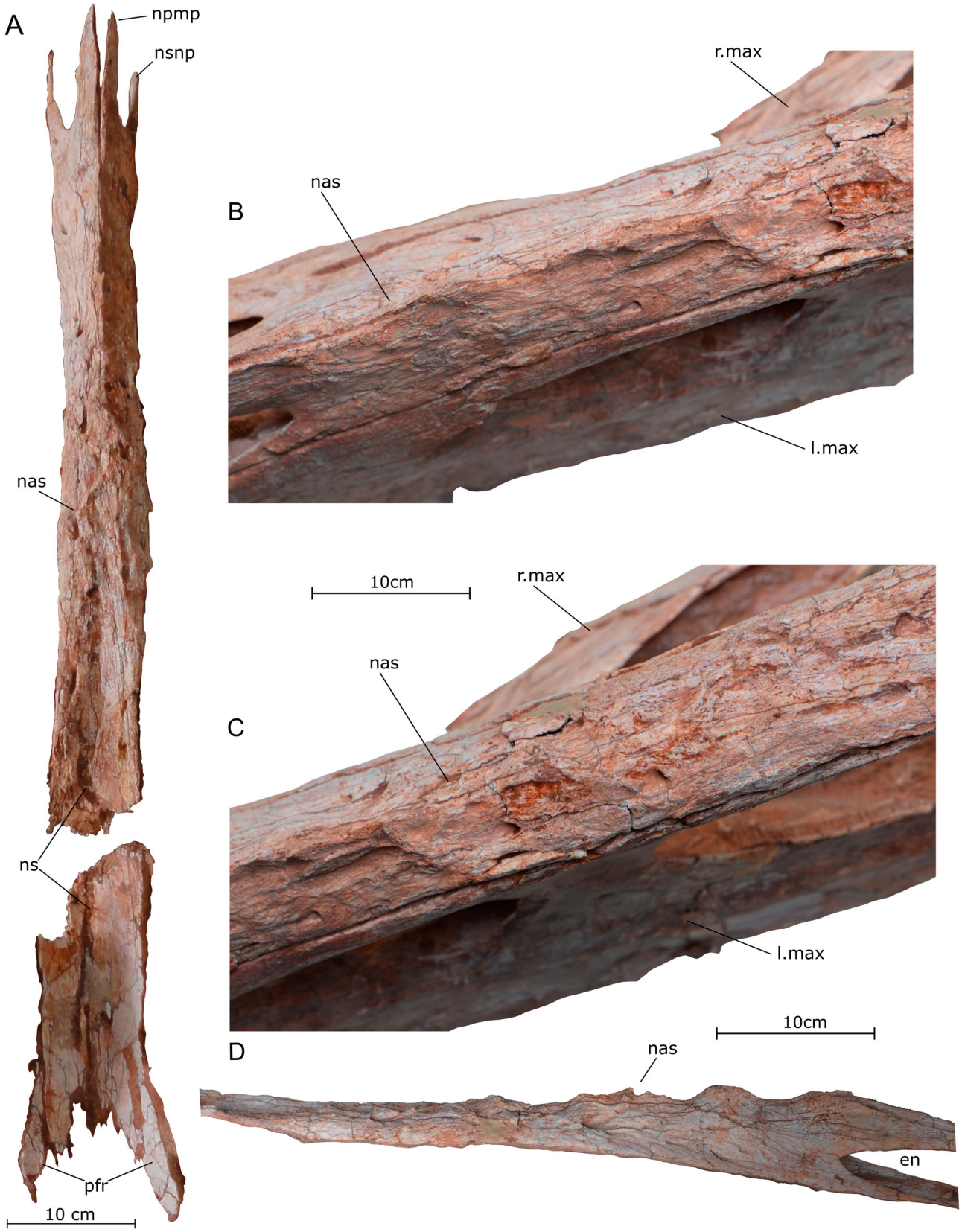

FIGURE 4. Nasals of the holotype specimen of *Qianzhousaurus sinensis* (GM F10004). **A**, conjoined nasals in dorsal view; **B**, close-up of the anterior nasal rugosities in dorsal view; **C**, close-up of the posterior nasal rugosities in dorsal view; **D**, nasal rugosities in right lateral view. **Abbreviations**: **en**, external naris; **l. max**, left maxilla; **nas**, nasal; **npmp**, nasal/premaxillary process; **ns**, nasal suture; **nsnp**, nasal sub-narinal process; **pfr**, prefrontals; **r. max**, right maxilla.

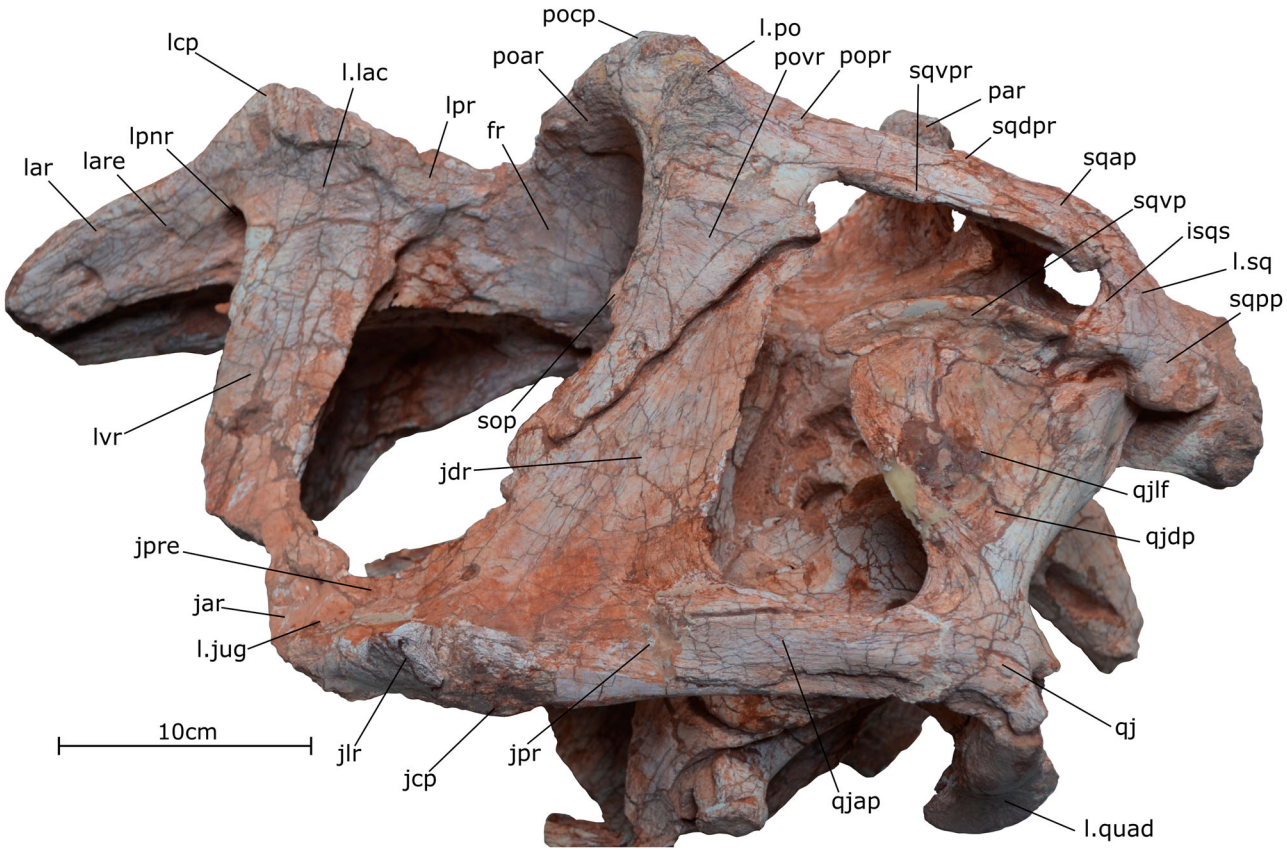

FIGURE 5. Posterior skull of the holotype specimen of *Qianzhousaurus sinensis* (GM F10004). Photograph of posterior skull in left lateral view. **Abbreviations**: **fr**, frontals; **isqs**, inter-squamosal sinus; **jar**, jugal anterior ramus; **jcp**, jugal cornual process; **jdr**, jugal dorsal ramus; **jlr**, jugal lateral rugosity; **jpr**, jugal posterior ramus; **jpre**, jugal pneumatic recess; **l. jug**, left jugal; **l. lac**, left lacrimal; **l. po**, left postorbital; **l. quad**, left quadrate; **lar**, lacrimal anterior ramus; **lare**, lacrimal accessory recess; **lcp**, lacrimal corneal process; **lpnr**, lacrimal pneumatic recess; **lpr**, lacrimal posterior ramus; **lsq**, left squamosal; **lvr**, lacrimal ventral ramus; **par**, parietal; **poar**, postorbital anterior ramus; **pocp**, postorbital cornual process; **popr**, postorbital posterior ramus; **povr**, postorbital ventral ramus; **qj**, quadratojugal; **qjap**, quadratojugal anterior process; **qjdp**, quadratojugal dorsal process; **qjlf**, quadratojugal lateral fossa; **r. sq**, right squamosal; **sop**, sub-orbital plate; **sqap**, squamosal anterior process; **sqdpr**, squamosal dorsal prong; **sqpp**, squamosal posterior process; **sqvp**, squamosal ventral process; **sqvpr**, squamosal ventral prong.

of the premaxilla act to orient the external naris more horizontally than in large derived taxa such as *Tyrannosaurus* (Brochu, 2003) and *Tarbosaurus* (Maleev, 1974; Hurum and Sabath, 2003), which exhibit an external naris that descends anteroventrally at a higher angle. Unlike in *Tarbosaurus*, which has an almost horizontal premaxilla-nasal suture that is immediately dorsal to the most anterior point of the external naris (Maleev, 1974; Hurum and Sabath, 2003; SLB pers. obs. PIN 4216/3), the same contact in *Q. sinensis* is positioned further posteriorly at around the mid-point of the dorsal surface of the external naris. The *Tarbosaurus* condition is also characteristic of *Tyrannosaurus* (Osborn, 1912), whereas albertosaurines (Carr, 1999; Currie, 2003) and the more basal large-bodied tyrannosauroid *Bistahieversor* (Carr and Williamson, 2010) are more similar to *Qianzhousaurus.* Anterior to the external naris, the lateral surface of the premaxilla is pierced by an accessory foramen (Fig. 2). This foramen is present on both the left and right premaxillae, although on the right bone the foramen is split into two smaller circular features, whereas it is a single, larger, ovoid foramen on the left. This feature is present in *Tyrannosaurus* (Brochu, 2003), *Tarbosaurus* (SLB pers. obs. PIN 4216/3), and *Gorgosaurus* (Lambe, 1917), for example.

The premaxilla houses four alveoli that are oriented mediolaterally, forming a wide U-shaped snout in which the teeth are all visible in anterior view, as is characteristic of tyrannosaurids (Brusatte et al., 2010; Carr and Williamson, 2010).

Maxilla—Both the right and left maxillae are present (Fig. 1) and well-preserved and consist of three processes: the main body (Fig. 2), the ventral ramus (Fig. 2) and the posterior ramus (Fig. 2), the latter two of which diverge from the body to form the anterior margin of the antorbital fenestra (Fig. 1).

The maxillae are elongate and low relative to most other tyrannosaurids, as is the case in *A. altai* (Brusatte et al., 2012:figs. 6, 7) and in the reconstructed cranium of *A. remotus* (Kurzanov, 1976). It is the elongate maxilla, plus nasal and anterior palate, that largely define the longirostrine skull morphology of these taxa. Juvenile tyrannosaurids generally have longer and lower maxillae than adults, the latter of which have deeper craniofacial regions (e.g., Carr, 1999).

The main body of the maxilla (Fig. 2) is convex along the tooth row, as in derived large-bodied tyrannosauroids (e.g., Sereno et al., 2009; Brusatte et al., 2010; Carr and Williamson 2010; Brusatte and Carr, 2016), although it is considerably less convex than in *Tyrannosaurus* and *Tarbosaurus.* The lateral surfaces of both left and right maxillae are rugose, more so than in *A. altai* (Brusatte et al., 2012) (Fig. 2), but not to the same degree as in *Tyrannosaurus* and *Tarbosaurus* (e.g., Brochu, 2003; Hurum and Sabath, 2003). Minor rugosity exists towards the ventral

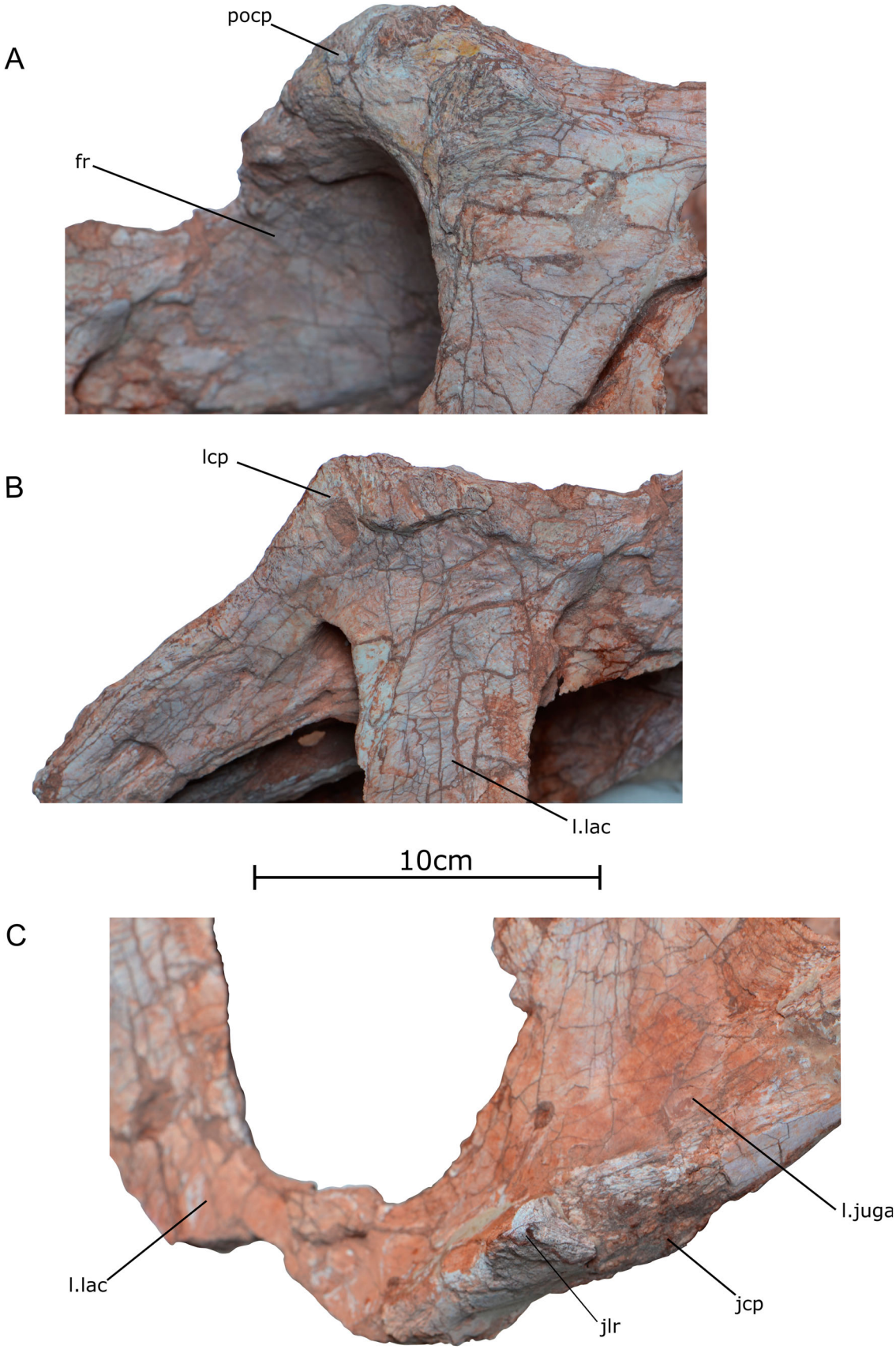

FIGURE 6. Cranial ornaments of the holotype specimen of *Qianzhousaurus sinensis* (GM F10004). **A**, photograph of left postorbital cornual process in left lateral view; **B**, photograph of left lacrimal cornual process in left lateral view; **C**, photograph of left jugal cornual process and lateral rugosity in left lateral view. **Abbreviations**: **fr**, frontals; **jcp**, jugal cornual process; **jlr**, jugal lateral rugosity; **l. jugal**, left jugal; **l. lac**, left lacrimal; **lcp**, lacrimal cornual process; **pocp**, postorbital cornual process.

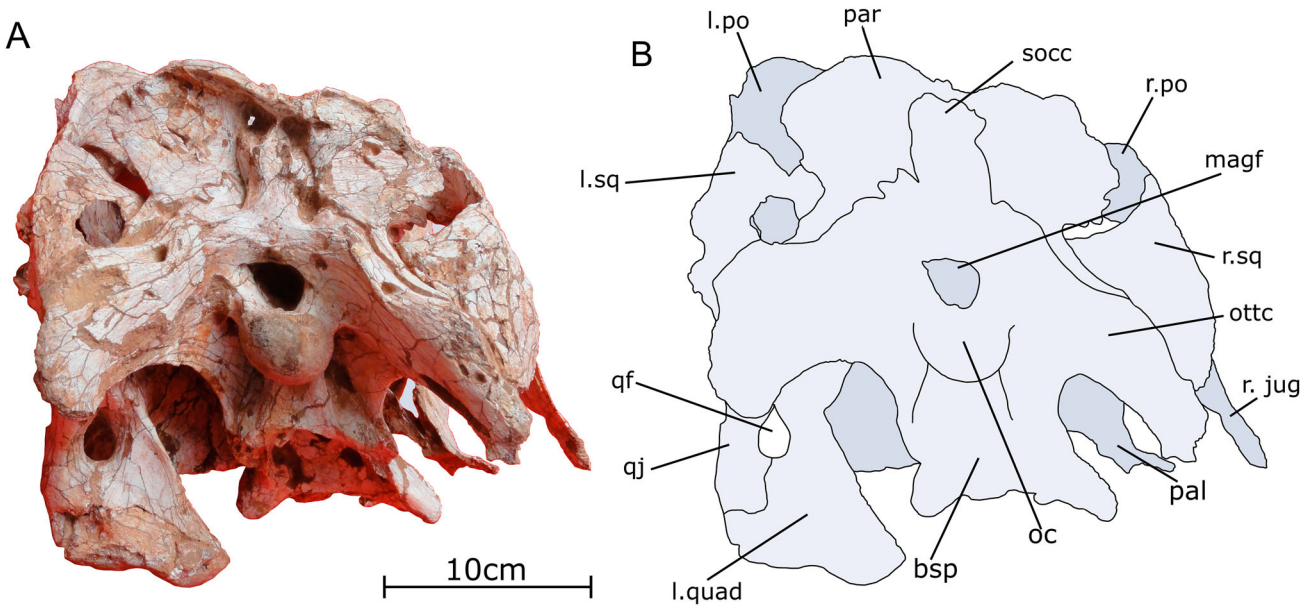

FIGURE 7. Occipital region of the skull of the holotype specimen of *Qianzhousaurus sinensis* (GM F10004). **A**, photograph of skull in posterior view; **B**, line drawing of skull in posterior view. **Abbreviations**: **bsp**, basisphenoid; **l. po**, left postorbital; **l. quad**, left quadrate; **l. sq**, left squamosal; **magf**, magnum foramen; **oc**, occipital condyle; **ottc**, otoccipital; **pal**, palatine; **par**, parietal; **pot**, postorbital tab; **qf**, quadrate foramen; **qj**, quadratojugal; **r. jug**, right jugal; **r. po**, right postorbital; **r. sq**, right squamosal; **socc**, supraoccipital.

margin of the maxilla and is accompanied by two rows of neurovascular foramina; one that follows the ventral margin of the tooth row and one that traverses centrally within the main body (Figs. 1, 2). There is an accumulation of these foramina slightly anterior to the maxillary fenestra, as is the case in *Tyrannosaurus* and *Tarbosaurus* (Hurum and Sabath, 2003).

The remaining two processes, the dorsal and ventral rami, are elongate, and extend posterodorsally and posteriorly, respectively. The dorsal ramus (Fig. 2) is bordered dorsally by the nasal for most of its length, and contacts the lacrimal posteriorly. In this way, the dorsal ramus of the maxilla forms the anterior portion of the dorsal margin of the antorbital fenestra.

The ventral process (Fig. 2) forms the posterior end of the maxillary tooth row before continuing as a thin projection that contacts the jugal at approximately the midpoint of the ventral rim of the antorbital fenestra. As the ventral ramus extends posteriorly, it loses the convex profile that begins on the ventral margin of the main body and becomes shallowly concave towards its posterior tip.

The maxillary fenestra (Figs. 1, 2) is located between the body of the maxilla and the ascending process. The fenestra is large and elongate, in the shape of an oval, which is also the case in *Alioramus altai* (Brusatte et al., 2009, 2012), but which differs from the proportionally much less anteroposteriorly ovoid, and more circular, shape in other tyrannosaurids. Anterior to the maxillary fenestra of *Qianzhousaurus* is a depression, which houses a small promaxillary fenestra (Figs. 1, 2), which is visible in lateral view and not concealed by the ascending ramus. This fenestra is smaller, and located much closer to the maxillary fenestra, than in *Alioramus altai* (Brusatte et al., 2012). There is no accessory depression located posterodorsal to the promaxillary fenestra; this additional opening is autapomorphic of *Alioramus altai* (Brusatte et al., 2009, 2012).

The ascending ramus of the maxilla is pierced, on both sides of the skull, by an elongate, ovoid accessory pneumatic fenestra, posterodorsal to the maxillary fenestra (Figs. 1, 2). This is not present in *Alioramus altai*, which instead possesses a shallower depression in this area, nor in any other tyrannosauroids, and thus was considered autapomorphic for *Qianzhousaurus* (Lü et al., 2014). The accessory fenestra is shaped and positioned differently on the two sides of the skull: on the left it is more ovoid and closer to the dorsal edge of the maxilla ascending ramus, on the right it is more of a discrete rectangular window that is positioned more centrally on the ascending ramus. Finally, we note an additional pneumatic feature of the maxilla that was not mentioned by Lü et al. (2014): a small fossa positioned between the anterior margin of the antorbital fenestra and the posterior margin of the maxillary fenestra (Figs. 1, 2). This is not present in *Alioramus altai* (Brusatte et al., 2012). In the derived tyrannosaurines *Tyrannosaurus* (Brochu, 2003), *Tarbosaurus* (Hurum and Sabath, 2003), and *Zhuchengtyrannus* (Hone et al., 2011), there is an accessory fenestra which pierces the maxilla in this region (Brusatte and Carr, 2016:character 328). *Qianzhousaurus* does not have a fenestra, but the fossa may be homologous.

The maxillary tooth row (Fig. 3C, D) includes 15 alveoli, which are incrassate in shape, with a labiolingual width 60% or greater than mesiodistal length. This corresponds to the intermediate condition of a phylogenetic character (Brusatte and Carr 2016: character 201 and references therein), shared with tyrannosaurids such as *Albertosaurus* and *Daspletosaurus*, but differing from the much thinner alveoli of *Alioramus altai* and the much thicker alveoli of *Tyrannosaurus* and *Tarbosaurus*, whose width is nearly equal to length. Thus, the dentition of *Qianzhousaurus* is moderately incrassate. The alveoli in *Qianzhousaurus* possess strongly convex mesial and distal margins, and straight to slightly convex labial and lingual margins. This is unlike the almost rectangular alveoli in *A. altai*, which are pinched labiolingually (Brusatte et al., 2012).

Nasal—The left and right nasals (Figs. 1–4) are fused as in tyrannosauroids generally, such that the internarial suture (Fig. 4) is almost completely obliterated, and the conjoined nasals form a vaulted structure as in derived tyrannosauroids (Holtz, 2001; Snively et al., 2006). In concert with the overall lengthening of the snout, the nasals are anteroposteriorly elongate and shallow dorsoventrally, compared with the deeper and anteroposteriorly stouter nasals in large, deep-snouted tyrannosaurids

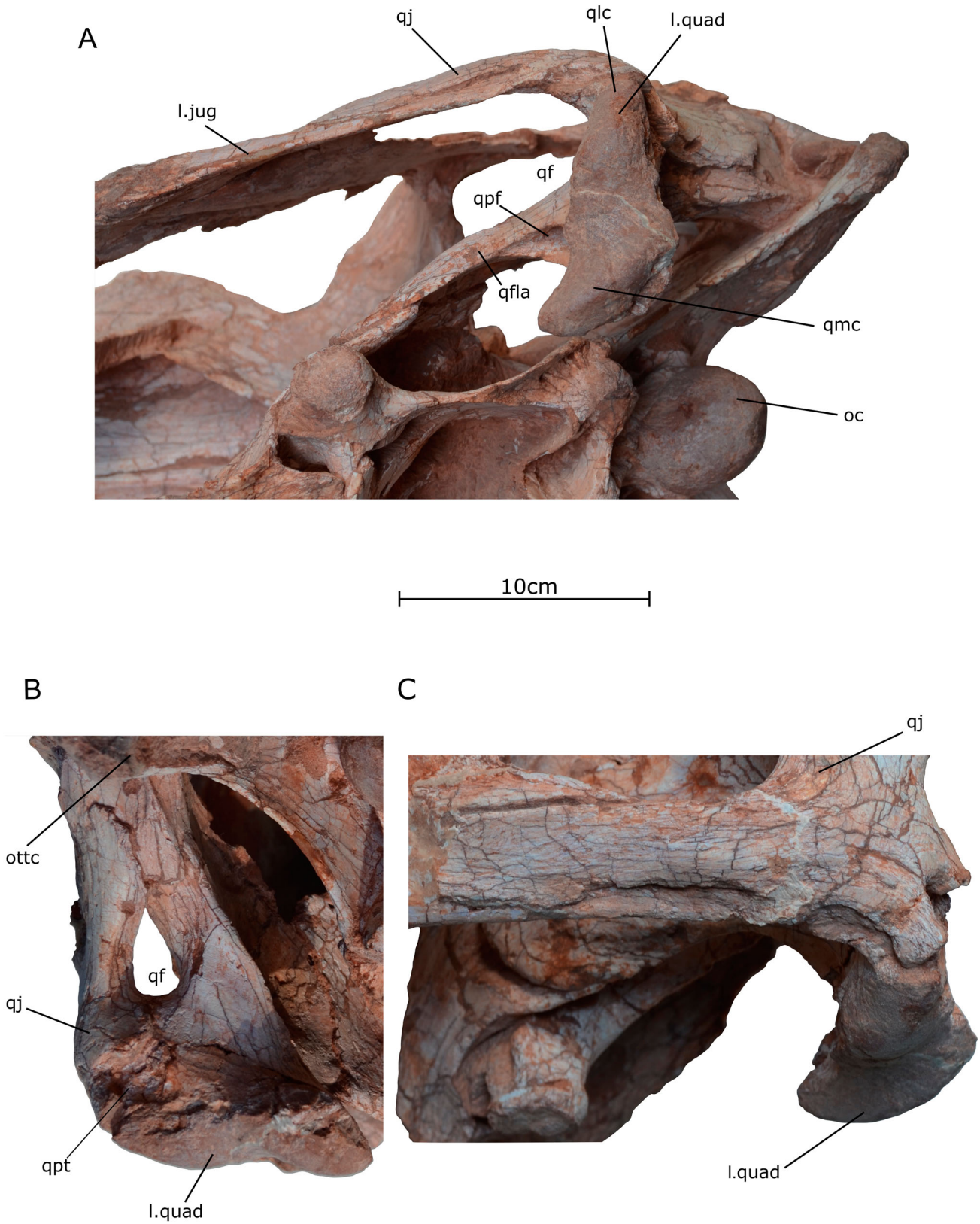

FIGURE 8. Close-ups of the quadrate and quadratojugal of the holotype specimen of *Qianzhousaurus sinensis* (GM F10004). **A**, photograph of posterior skull in ventral view; **B**, photograph of the left quadratojugal and left quadrate in posterior view; **C**, photograph of the left quadratojugal and left quadrate in oblique lateral view. **Abbreviations**: **l. jug**, left jugal; **l. quad**, left quadrate; **oc**, occipital condyle; **ottc**, otoccipital; **qf**, quadrate foramen; **qfla**, quadrate flange, **qj**, quadratojugal; **qlc**, quadrate lateral condyle; **qmc**, quadrate medial condyle; **qpf**, quadrate pneumatic foramen; **qpt**, quadratojugal posterior tab.

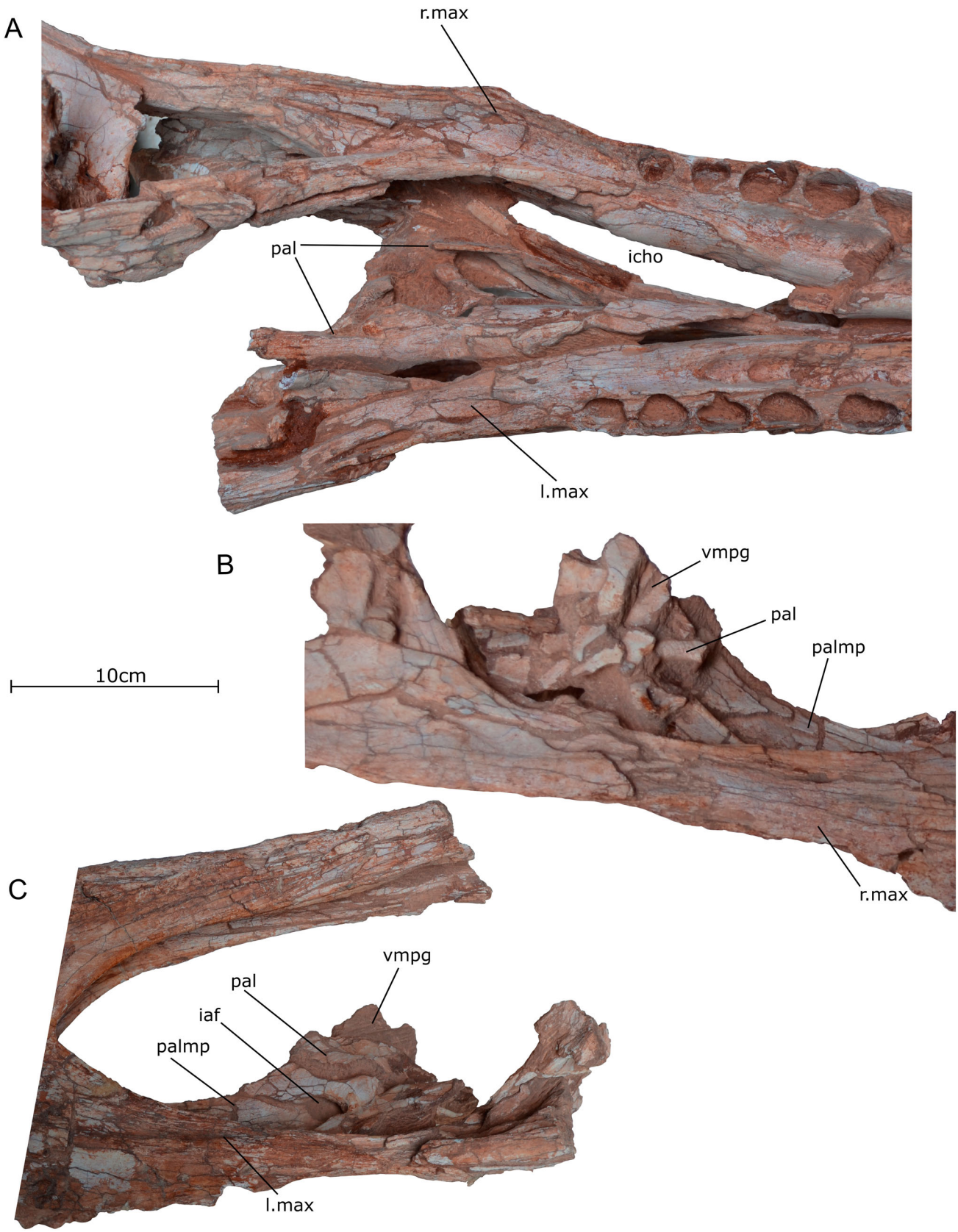

FIGURE 9. Close-ups of the palatines of the holotype specimen of *Qianzhousaurus sinensis* (GM F10004). **A**, photograph of palatines in ventral view; **B**, photograph of right palatine in right lateral view; **C**, photograph of left palatine in left lateral view. **Abbreviations**: **iaf**, internal antorbital fossa; **icho**, internal choana; **l. max**, left maxilla; **pal**, palatine; **palmp**, palatine maxillary process; **r. max**, right maxilla; **vmpg**, vomopterygoid process.

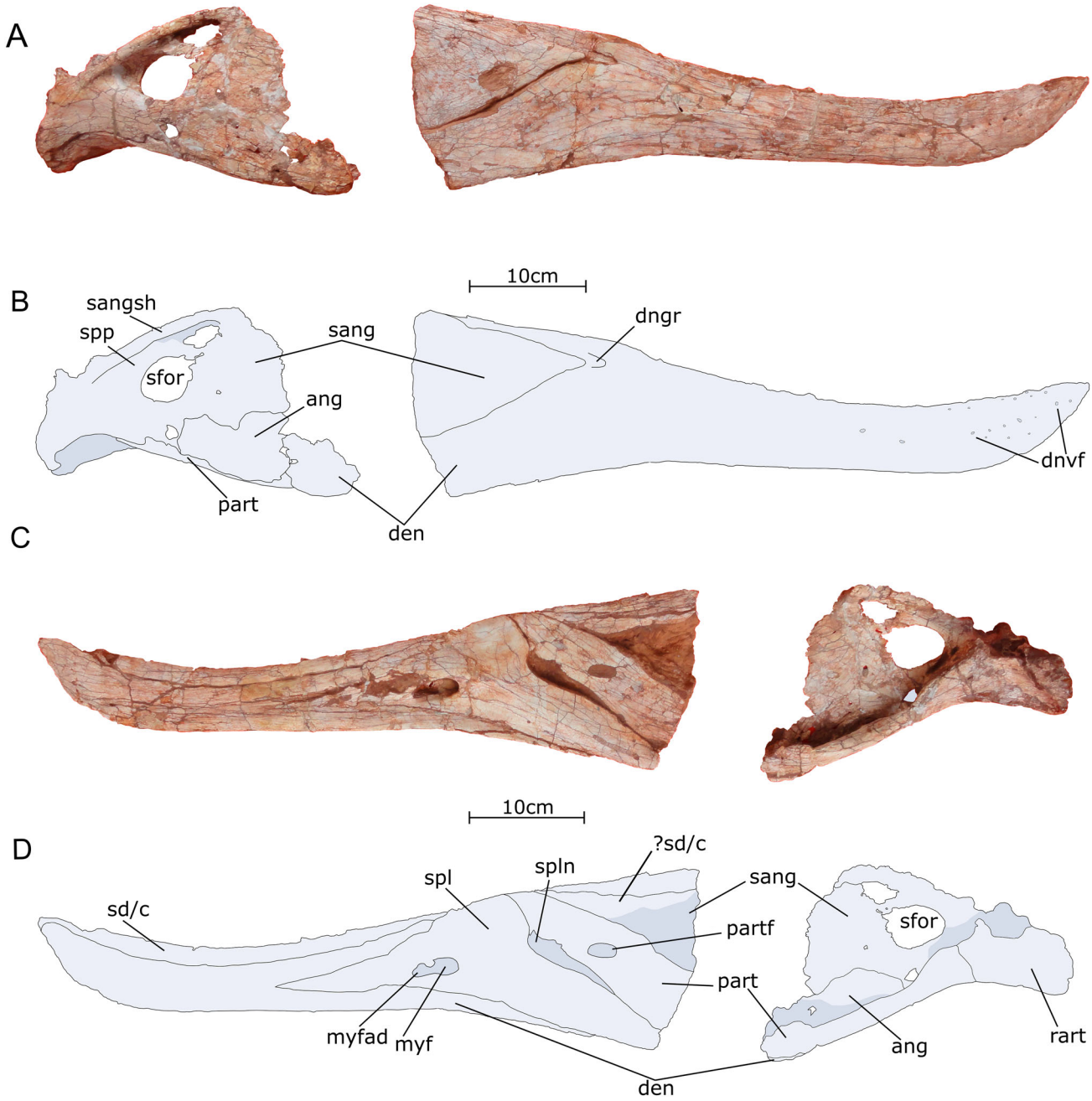

FIGURE 10. Right mandible of the holotype specimen of *Qianzhousaurus sinensis* (GM 10004). **A**, photograph of the right mandible in right lateral view; **B**, line drawing of the right mandible in right lateral view; **C**, photograph of the right mandible in medial view; **D**, line drawing of the right mandible in medial view. **Abbreviations**: **ang**, angular; **den**, dentary; **dngr**, dentary groove; **dnvf**, dentary neurovascular foramina; **myf**, mylohyoid foramen; **myfad**, mylohyoid accessory depression; **part**, prearticular; **partf**, prearticular fossa; **rart**, retroarticular; **sang**, surangular; **sangsh**, surangular shelf; **sd/c**, supradentary coronoid; **?sd/c**, possible posterior extension of the coronoid; **sfor**, surangular foramen; **spl**, splenial; **spln**, splenial notch; **spp**, surangular pneumatic pocket.

such as *Tyrannosaurus* (Brochu, 2003) and *Tarbosaurus* (Maleev, 1974).

The nasals overlie nearly the entire length of the maxilla, and the long, nearly straight suture is clearly marked in lateral view (Fig. 2). The nasal-maxilla suture is tilted in an anteroposterior-posterodorsal direction, but the angle of incline is much lower than in large, deep-snouted tyrannosaurids like *Tyrannosaurus* (Brochu, 2003) and *Tarbosaurus* (Maleev, 1974; Hurum and Sabath, 2003). In lateral view (Fig. 4D), the dorsoventral depth of the nasal decreases steadily in a posterior direction, tapering into a thin plate of bone that contacts the lacrimals, prefrontals, and frontals. This contact is visible nearly exclusively in dorsal view (Fig. 3A, B), and is described below. As in *Alioramus altai* (Brusatte et al., 2009, 2012; Gold et al., 2013) and deep-snouted tyrannosaurids, there is no evidence of external pneumaticity on the lateral surface of the nasal, nor does the smooth antorbital fossa extend onto the nasal. In more basal tyrannosauroids, however, the nasals are internally pneumatized, via

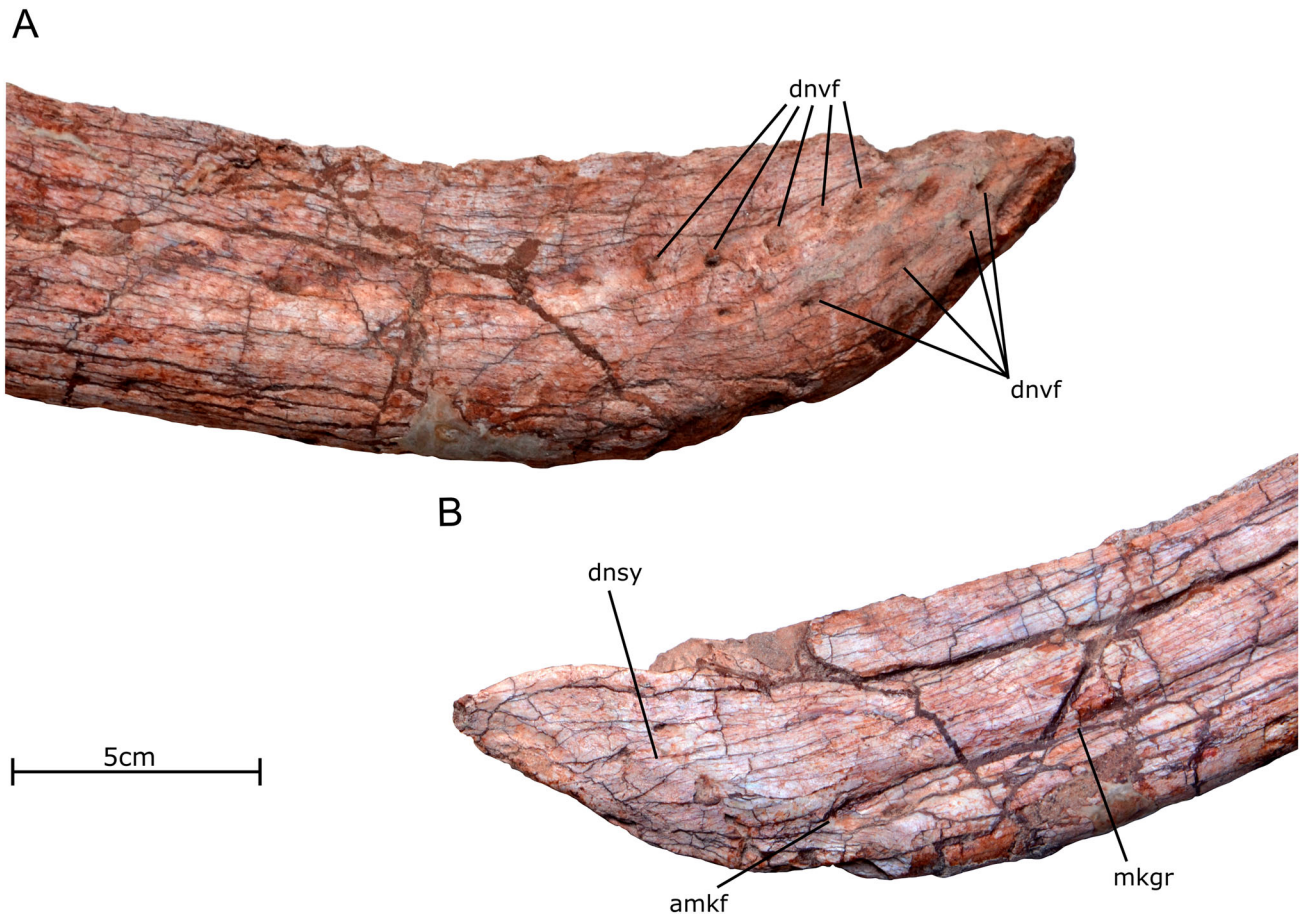

FIGURE 11. Anterior tip of the dentary of the holotype specimen of *Qianzhousaurus sinensis* (GM F10004). **A**, photographs of dentary tip in right lateral view; **B**, photograph of right dentary tip in medial view. **Abbreviations**: **amkf**, anterior Meckelian fossa; **dnsy**, dentary symphysis; **dnvf**, dentary neurovascular foramina; **mkgr**, Meckelian groove.

an external pneumatic foramen within a portion of the antorbital fossa that extends onto the nasal (e.g., *Eotyrannus*: Hutt et al., 2001; *Dilong*: Xu et al., 2004; *Guanlong*: Xu et al., 2006; *Yutyrannus*: Xu et al., 2012).

Anteriorly the nasals bifurcate to form the posterior corner of the external naris. The bifurcation is comprised of two projections. First, a large premaxillary process extends anteriorly to meet the dorsal ramus of the premaxilla, forming the dorsal border of the naris (Fig. 4). Second, a short subnarial process continues ventrally underneath the naris to overlap the maxilla, forming a small portion of the floor of the naris (Fig. 4). On the left side of the skull, the subnarial process does not appear to meet the premaxilla anteriorly, leaving the maxilla to form much of the narial floor, but this may be an artifact of breakage. On the right side, the subnarial process either meets or nearly meets the premaxilla. This contact is not evident in lateral view, where it is obscured by the lateral surface of the maxilla underneath the naris but is visible in dorsal view.

In dorsal view, the nasals are essentially a straight rod, whose mediolateral width remains nearly constant across the entire element (Fig. 4A). This is also the case in *Alioramus remotus*, *Alioramus altai*, albertosaurines and non-tyrannosaurid tyrannosauroids (Brusatte et al., 2010; Brusatte and Carr, 2016:character 41), differing from the condition in most *Daspletosaurus*, *Tyrannosaurus*, and *Tarbosaurus* specimens, where the conjoined nasals taper in width posteriorly. With that said, there is some variation within the 'straight' condition: the nasals are properly straight in *Qianzhousaurus*, with nearly linear lateral margins on left and right sides, whereas in both *Alioramus* species the lateral margins are moderately concave due to slight anterior and posterior expansions, giving the fused nasal element a stretched hourglass shape in dorsal view. This properly straight condition might be an autapomorphy of *Qianzhousaurus*; it was not recognized by Lü et al. (2014). We do note, however, that this may be a particularly variable feature; *Gorgosaurus*, for instance, is polymorphic: the standard hourglass shape is seen in some specimens (e.g., ROM 1247), whereas at least one specimen is straight (CMN 2120; Carr, 1999).

Posteriorly, the nasals contact the lacrimals, prefrontals, and frontals. In comparison to large, deep-snouted tyrannosaurids like *Tyrannosaurus* (Brochu, 2003) and *Tarbosaurus* (Maleev, 1974; Hurum and Sabath, 2003), the nasal-lacrimal contact in *Q. sinensis* is exceedingly dorsoventrally thin in lateral view. Thus, this suture is best seen in dorsal view, as a nearly straight line abutting the medial margin of the lacrimal (Fig. 3A, B). At their most posterior extent, the nasals splay into two short rami on the left and right sides of the conjoined element (Fig. 4A), separated by a medial region of jagged interlocking sutures. These features—visible only in dorsal view—comprise the contacts with the frontals (Fig. 3A, B) and small prefrontals (Fig. 4). The two rami in *Q. sinensis* are longer and project further posteriorly than those of *A. altai* (Brusatte et al., 2012:fig. 10), in which the rami are indistinguishable from the jagged central region between them; this, however, may be an artifact of breakage in the latter taxon.

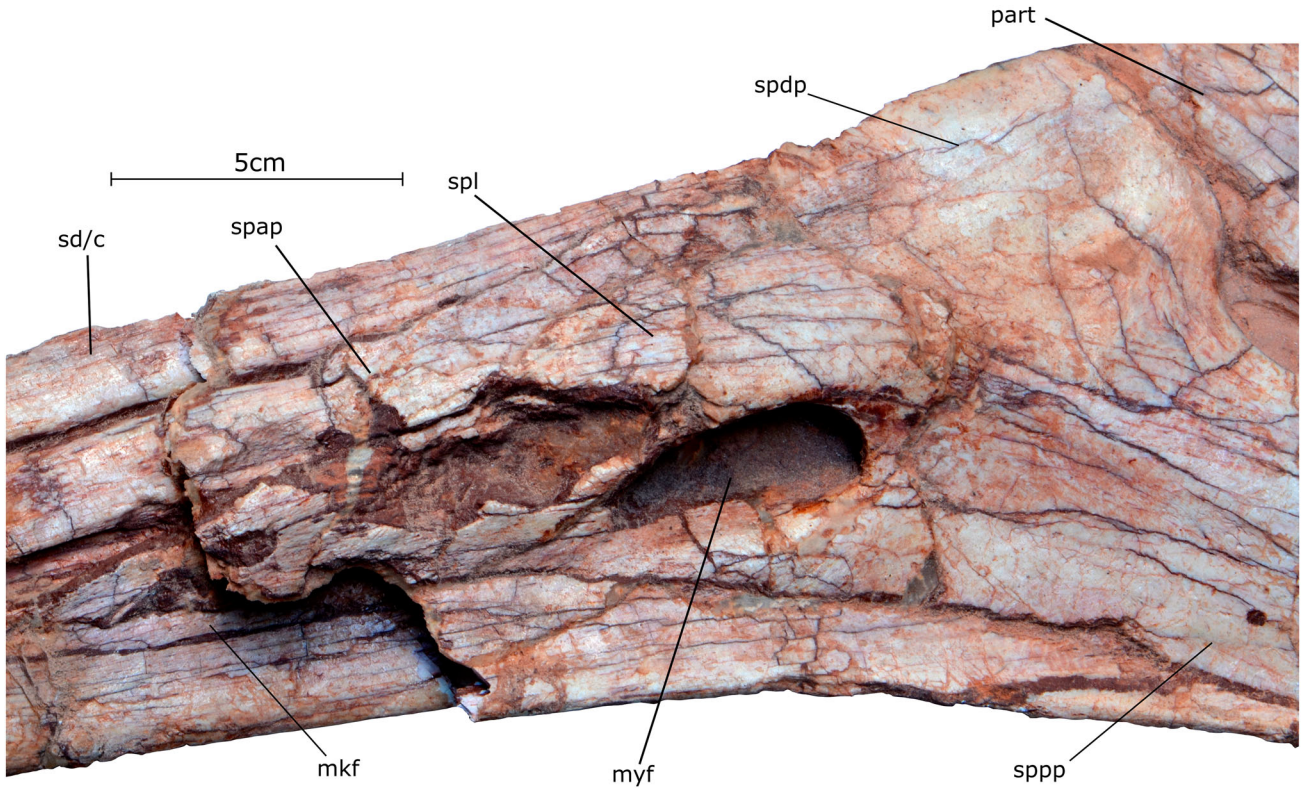

FIGURE 12. Splenial and surrounding bones of the holotype specimen of *Qianzhousaurus sinensis* (GM 10004). **Abbreviations**: **mkf**, Meckelian fossa; **myf**, mylohyoid foramen; **part**, prearticular; **sd/c**, supradentary coronoid; **spl**, splenial; **spap**, splenial anterior process; **sppp**, splenial posterior process; **spdp**, splenial dorsal process.

The most salient feature of the nasals is the extensively rugose surface texture, particularly on the dorsal surface (Fig. 4). Among the overall roughened and blistered texture, a series of four pronounced, rugose mounds stand out from the dorsal surface of the midline of the fused nasal element. The sculptured nasal surface is seen in other tyrannosaurids, but is especially pronounced in alioramins, and the discrete midline rugosities are a synapomorphy of Alioramini, seen also in *Alioramus remotus* and *Alioramus altai* (Lü et al., 2014; Brusatte and Carr, 2016). The midline rugosities are larger, smoother, and more hillock-shaped compared with the slightly smaller, rugged mounds of the *Alioramus altai* specimen described by Brusatte et al. (2009, 2012), although this may be because the *Qianzhousaurus* holotype is more mature. Another nasal indicator of greater maturity in the *Qianzhousaurus* holotype compared with the *Alioramus altai* holotype is the more open suture between the left and right nasals in the latter, which continues farther anteriorly from the posterior end of the bone as a cleft (see the supplemental information of Lü et al., 2014).

Lacrimal—Both left and right lacrimals are present. The left lacrimal (Fig. 1) is nearly complete, but the right (Fig. 1) is broken along its ventral ramus, leaving only the dorsal portion of the bone, plus a small portion ventrally articulated with the maxilla and jugal. As in *Alioramus altai* and some other derived tyrannosaurids such as *Tyrannosaurus* (Molnar, 1991; Brochu, 2003) and *Tarbosaurus* (Hurum and Sabath, 2003) the lacrimal in *Qianzhousaurus* is shaped like the number 7, with elongate anterior (Fig. 5) and ventral rami (Fig. 5) that meet at an acute angle. These rami define the posterodorsal region of the antorbital fenestra, and the ventral ramus separates the fenestra from the orbit. There is also a small posterior ramus (Fig. 5) that projects backwards to form the anterodorsal corner of the orbit.

The ventral ramus (Fig. 5) extends anteroposteriorly when in articulation with the other skull bones, differing slightly from the more vertical orientation in *Alioramus altai* (Brusatte et al., 2009, 2012), *Tyrannosaurus* (Brochu, 2003), *Tarbosaurus* (Hurum and Sabath, 2003), and other large tyrannosaurids (e.g., Currie, 2003). This may be a potential autapomorphy of *Qianzhousaurus*, but it is difficult to rule out the effect of taphonomic distortion and ontogenetic variation (Tsuihiji et al., 2011; Carr, 2020).

The lacrimal is highly pneumatic, as is standard for tyrannosauroids (e.g., Gold et al., 2013). The most prominent pneumatic feature externally is a large lacrimal recess (Fig. 5), a funnel-like opening at the posterodorsal corner of the antorbital fossa, where the lacrimal anterior and ventral rami diverge. It is deep and well-defined, and partitioned internally by an arcuate ridge, as in *Alioramus altai* (Brusatte et al., 2012). There is also at least one accessory recess anterior to the lacrimal recess on the anterior ramus (Fig. 5), but poor preservation makes it difficult to determine if there were one or two accessory openings; this feature is highly variable phylogenetically and ontogenetically in tyrannosaurids (Brusatte et al., 2012).

Perched above the lacrimal recess, on the dorsal surface of the bone, is a pronounced cornual process, or 'lacrimal horn' (Figs. 5, 6). It projects markedly from the skull roof, as a large and rugose mound, whose peak is approximately dorsal to the level of the ventral ramus. It also is swollen laterally, such that it overhangs the orbit in dorsal view. There is great variability in the shape and position of this process in tyrannosauroids. It is expressed as a small, conical horn in *Alioramus altai* (Brusatte et al., 2009, 2012); compared with this condition, the cornual process of *Qianzhousaurus* is larger, more swollen, and more laterally overhanging, which is likely a sign of greater maturity of the

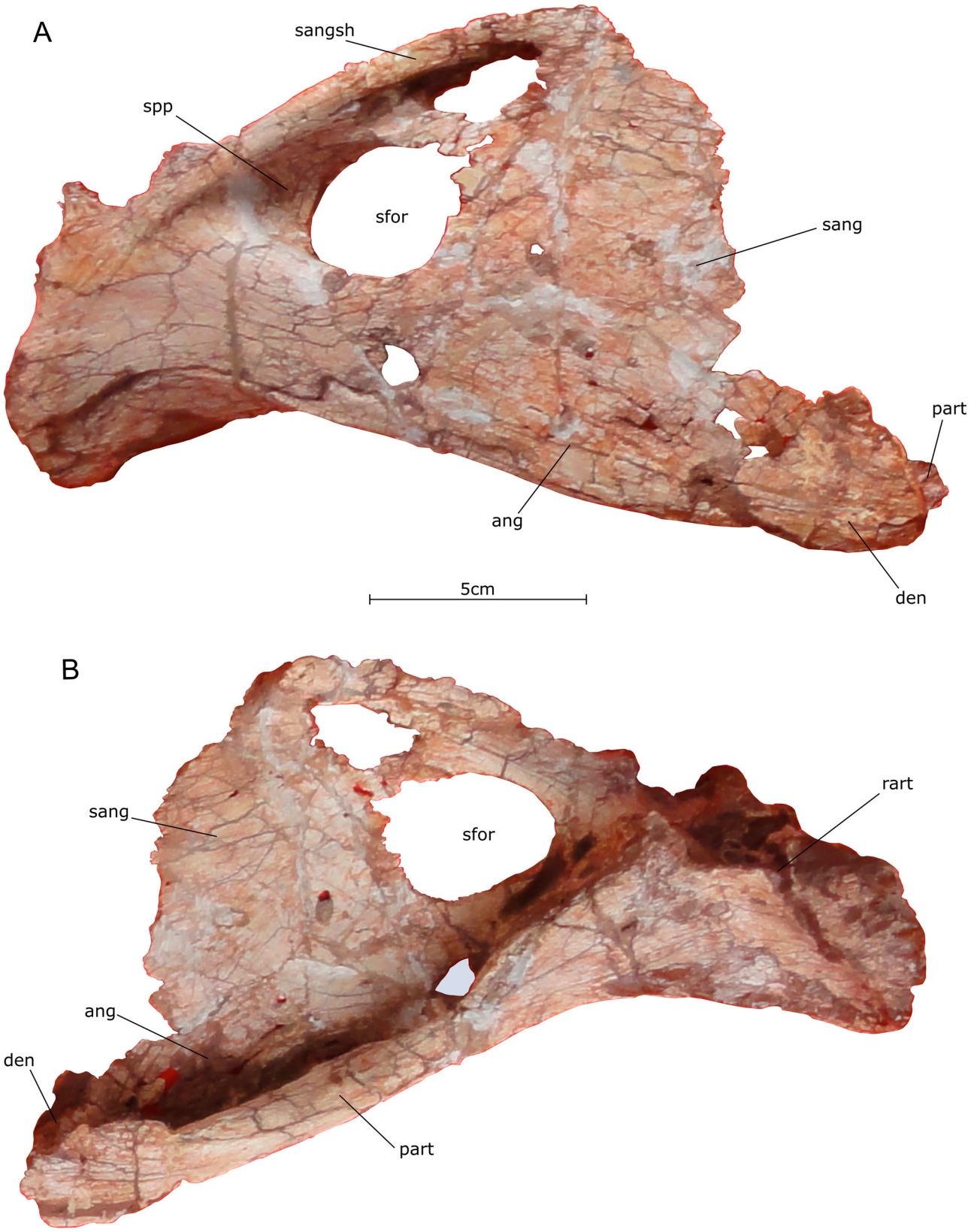

FIGURE 13. Posterior end of the right mandible of the holotype specimen of *Qianzhousaurus sinensis* (GM 10004). **A**, photograph of the posterior right mandible in right lateral view; **B**, photograph of the posterior right mandible in medial view. **Abbreviations**: **ang**, angular; **den**, dentary; **part**, prearticular; **rart**, retroarticular; **sang**, surangular; **sangsh**, surangular shelf; **sfor**, surangular foramen; **spp**, surangular pneumatic pocket.

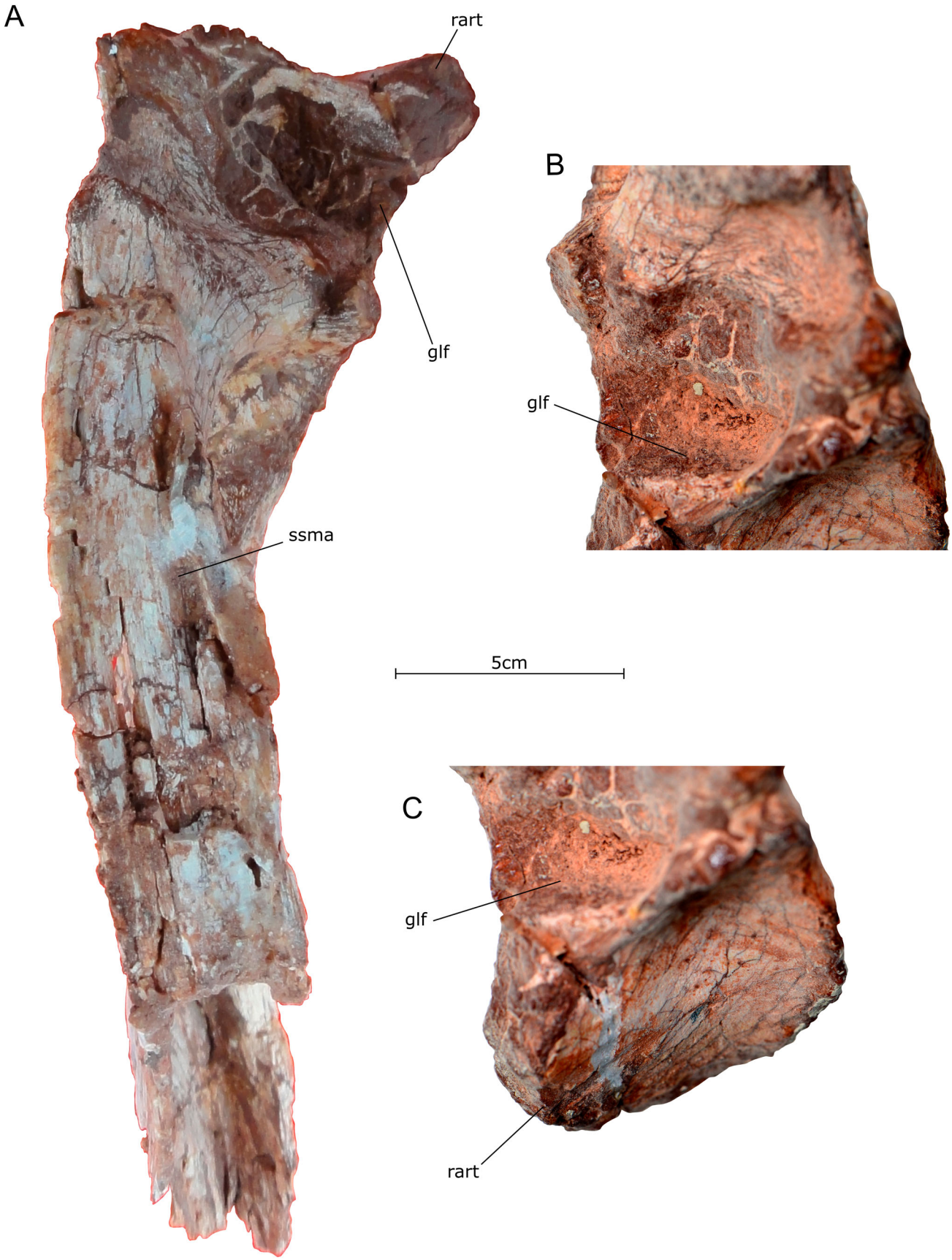

FIGURE 14. Articular region of the right mandible of the holotype specimen of *Qianzhousaurus sinensis* (GM 10004). **A**, photograph of the mandible articular region in dorsal view; **B**, photograph of the glenoid fossa in dorsal view; **C**, photograph of the retroarticular region in dorsal view. **Abbreviations**: **glf**, glenoid fossa; **rart**, retroarticular process; **ssma**, surrangular shelf muscle attachment.

Qianzhousaurus holotype vs. the *Alioramus altai* holotype (Lü et al., 2014). In adult *Tyrannosaurus* (Brochu, 2003) and *Tarbosaurus* (Hurum and Sabath, 2003), however, the cornual process is essentially absent, as it is so inflated that it has merged with the remainder of the dorsal lacrimal (Brusatte and Carr, 2016:character 316).

Jugal—Both left (Figs. 1, 3–5) and right (Figs. 1, 2) jugals are present but incomplete. The jugal is composed of three main processes: an anterior ramus (Fig. 5) that contacts the lacrimal and maxilla, a dorsal ramus (Fig. 5) that articulates with the postorbital to form the posterior border of the orbit, and a posterior ramus (Fig. 5) overlapped by the quadratojugal (Fig. 5), where the two bones form the floor of the lateral temporal fenestra (Fig. 3A, B).

There are two prominent features on the jugal. The first is the cornual process (Figs. 5, 6), located along the ventral margin of the bone underneath the orbit. This structure is present in tyrannosauroids generally, but is especially pronounced in tyrannosaurids (e.g., Brusatte et al., 2010; Brusatte and Carr, 2016: character 76; Carr and Williamson, 2010). In addition, *Alioramus altai* was described as having an autapomorphic condition in which there is also a laterally projecting 'horn' on the jugal, above the standard cornual process (Brusatte et al., 2009, 2012). Lü et al. (2014) described *Qianzhousaurus* as 'lacking' the autapomorphic horn of *Alioramus*, but this is misleading. In fact, *Qianzhousaurus* does have a laterally projecting rugosity (Figs. 5, 6), but compared with the condition in *Alioramus*, it is larger, more swollen, more ridge-like than conical, more expansive anteroposteriorly, and it is peaked at its midpoint, so that only this portion projects strongly laterally. Although the rugosity of *Qianzhousaurus* does not have the discrete horn-like shape of *Alioramus*, we consider it a homologous structure, and note that discrete lateral projections are absent in other tyrannosaurids. In *Qianzhousaurus*, the surface of the rugosity is scoured by dorsoventrally inclined lineations, and associated with several foramina, for neurovasculature (Fig. 6C).

The jugal of *Qianzhousaurus* is pneumatized, but external pneumatic fossae and foramina are difficult to describe due to breakage and crushing. On the better preserved right jugal, there is a pneumatic recess on the lateral surface of the anterior ramus (Fig. 1B), in the posteroventral corner of the antorbital fossa, as in *Alioramus altai* and other tyrannosauroids, but its shape and structure are unclear. The jugal is generally flat and not inflated laterally, a sign that the internal recess does not voluminously fill the bone; this is also the case in *Alioramus altai* and juveniles of *Bistahieversor* and *Gorgosaurus*, whereas juvenile and adult *Tyrannosaurus*, *Tarbosaurus*, and *Daspletosaurus* exhibit inflated jugals (Brusatte et al., 2012).

The jugal widely contributes to the ventral floor of the orbit, which is weakly concave and approximately level with the jugal-lacrimal contact. This is also the case in *Alioramus altai* and tyrannosauroids generally, whereas the largest deep-skulled species such as *Tyrannosaurus* and *Tarbosaurus* have a deeper, more U-shaped orbital floor that extends further ventrally than the jugal-lacrimal suture (Sereno et al., 2009; Brusatte et al., 2010; Brusatte and Carr, 2016:character 79). Posterior to the orbit, the dorsal ramus of the jugal meets the postorbital via an elongated, anteroventral suture (Fig. 5). The dorsal ramus (Fig. 5) of the jugal is particularly anteroposteriorly broad and mediolaterally flat, compared with the thin and tapering dorsal ramus of *Alioramus altai* (Brusatte et al., 2012). These taxa—or at least their holotypes—differ in another important way: in *Alioramus altai* there is a shallow notch for the postorbital on the jugal dorsal ramus, whereas in *Qianzhousaurus* there is a deep, interlocking notch for the postorbital (Brusatte and Carr, 2016:character 72). In sum, *Qianzhousaurus* has a thicker, broader postorbital wall—comprised of the jugal dorsal ramus and postorbital ventral ramus—than *Alioramus altai*, which is probably a sign of greater maturity of the holotype.

Postorbital—Left (Figs. 1–5) and right (Fig. 1A, B) postorbitals are present and well preserved (Fig. 4). They exhibit the characteristic T-shape of most theropods, consisting of anterior, posterior, and ventral processes. In general, the postorbital of *Qianzhousaurus* is a stouter bone with thicker processes compared with the more gracile postorbitals of the holotypes of *Alioramus altai* (Brusatte et al., 2009, 2012) and *Alioramus remotus* (Kurzanov, 1976), and more closely resembles the postorbitals of mature individuals of large, deep-skulled taxa such as *Albertosaurus* (Currie, 2003), *Tarbosaurus* (Hurum and Sabath, 2003), and *Tyrannosaurus* (Molnar, 1991; Brochu, 2003).

The most distinctive aspect of the postorbital is the enlarged cornual process (Figs. 5, 6), which is expressed as a large swelling in the region where the anterior and ventral processes meet, above the posterodorsal corner of the orbit. It projects above the skull roof as a convex boss, as is the case in mature specimens of all other tyrannosaurids, but differing from the much gentler cornual processes of the *Alioramus altai* and *Alioramus remotus* holotypes, which are restricted to a raised rim at the posterodorsal corner of the orbit (Sereno et al., 2009; Brusatte et al., 2010; Brusatte and Carr, 2016:character 81). The surface of the cornual process in *Qianzhousaurus* is rugose and scored with lineations, and on the right side appears to be abutted posteriorly by a subtle fossa, although this could be an artifact of damage.

The anterior process (Fig. 5) extends forward and sweeps medially to contact the frontal, above the orbit. In dorsal view (Fig. 3A, B), the contact between the postorbital and frontal is anteroposteriorly long, and the trace of the suture is a triangular medial edge of the postorbital slotting into a concavity on the frontal. Much of the dorsal surface of the postorbital anterior process is excavated by the smooth supraorbital fossa, which extends medially and posteriorly onto the dorsal surface of the frontal. Viewed dorsally, the postorbital approaches the lacrimal but does not contact it, allowing the frontal to form the middle of the dorsal orbital margin. The frontal contribution to the orbital border is a small notch, as in *Alioramus altai*, *Teratophoneus*, *Albertosaurus*, and *Gorgosaurus*. In contrast, basal tyrannosauroids have a much broader frontal contribution to the orbital margin, whereas in derived deep-skulled tyrannosaurines such as *Daspletosaurus*, *Tarbosaurus*, and *Tyrannosaurus* the postorbital and lacrimal contact to exclude the frontal from the orbital margin, sometimes associated with a separate palpebral ossification (Sereno et al., 2009; Carr and Williamson, 2010; Brusatte et al., 2010; Brusatte and Carr, 2016:character 120).

The posterior process of the postorbital (Fig. 5) projects nearly straight posteriorly, without the dorsal curvature of *Alioramus altai* (Brusatte et al., 2012), to contact the squamosal to form the dorsal bar of the lateral temporal fenestra. The postorbital contribution to this bar is limited: the posterior end of the posterior process does not reach the posterior margin of the lateral temporal fenestra, but terminates anterior to it, at about 70% of the anteroposterior length of the fenestra. In this sense, *Qianzhousaurus* is more like *Albertosaurus* and *Gorgosaurus* than *Alioramus altai* and other tyrannosaurids, in which the posterior processes reach the back end of the fenestra (Brusatte and Carr, 2016:character 85; note *Qianzhousaurus* is scored incorrectly). At the corner where the ventral process and posterior process meet, a small tab-like flange of bone (Fig. 5) with rugose surface texture protrudes into the lateral temporal fenestra. This is not present in *Alioramus altai* (Brusatte et al., 2012), but is seen in some mature tyrannosaurids (e.g., *Albertosaurus*: Currie, 2003:fig. 8).

The ventral process of the postorbital (Fig. 5) overlaps the dorsal ramus of the jugal to form the postorbital bar. The ventral process in *Qianzhousaurus* is intermediate in morphology between that of *Alioramus altai* and that of other

derived tyrannosaurids such as *Albertosaurus*, *Gorgosaurus* (Currie, 2003), *Tyrannosaurus* (Molnar, 1991; Brochu, 2003), and *Tarbosaurus* (Hurum and Sabath, 2003). In *Alioramus altai*, this process is gracile, tongue-shaped, projects nearly straight ventrally, does not reach the floor of the orbit, and ends in a broadly rounded tip (Brusatte et al., 2012). In mature tyrannosaurids the ventral process is broad, oriented strongly anteroventrally, reaches or nearly reaches the orbital floor, and near its end gives rise to a suborbital (= subocular) process that projects into the orbit as a flange (e.g., Osborn, 1912; Brochu, 2003; Hurum and Sabath, 2003). In *Qianzhousaurus*, the ventral process does not reach the orbital floor, but it is broad and projects anteroventrally at a lower angle than in mature deep-skulled tyrannosaurids. The distal end of the ventral process has a suborbital process (Fig. 5), but it is incipient and takes the form of a small tab (Brusatte and Carr, 2016:character 86). Furthermore, the suborbital process is positioned at the ventral end of the ventral process, as in *Bistahieversor*, *Albertosaurus*, *Gorgosaurus*, and *Teratophoneus*, rather than set off from the ventral tip by a notch as in the derived deep-skulled tyrannosaurines *Daspletosaurus*, *Tarbosaurus*, and *Tyrannosaurus* (Brusatte and Carr, 2016:character 87).

Squamosal—Both the left and right squamosals are present; the left bone is complete and well preserved (Fig. 5), but the right is broken ventrally (Fig. 1A, B). The squamosal consists of three main processes visible in lateral view: an anterior process (Fig. 5) that forks anteriorly to meet the postorbital, a ventral process (Fig. 5) that extends into the lateral temporal fenestra to join the quadratojugal, and a posterior process that forms the posterodorsal corner of the skull (Fig. 5). In dorsal view, there is also a medial process that extends medially to contact the parietal and potentially the quadrate, forming the posterolateral region of the supratemporal fenestra.

The anterior process projects forward, with a slight dorsal sweep, to clasp the postorbital posterior process above the lateral temporal fenestra. The clasp is defined by dorsal and ventral prongs on the squamosal anterior process, both of which project anteriorly so that they approach but do not extend further than the anterior edge of the lateral temporal fenestra. This is incorrectly reconstructed by Lü et al. (2014:fig. 1), who showed both prongs as short structures terminating near the midpoint of the lateral temporal fenestra. In *Qianzhousaurus* the ventral prong (Fig. 5) is widely visible in lateral view, unlike in *Alioramus altai*, where the prong is similarly anteroposteriorly extensive but mostly hidden behind the postorbital posterior process when viewed laterally (Brusatte et al., 2012). Compared with other tyrannosaurids, including *Alioramus altai* (Brusatte et al., 2012) and deep-snouted species (e.g., Maleev, 1974; Brochu, 2003; Currie, 2003; Hurum and Sabath, 2003), the dorsal prong (Fig. 5) in *Qianzhousaurus* is noticeably gracile and shallow dorsoventrally. The depth of this process in tyrannosaurids is caused by a flange of bone that extends dorsal to the main body of the dorsal prong (Sereno et al., 2009; Brusatte et al., 2010; Brusatte and Carr, 2016:character 97). This flange is present in *Qianzhousaurus*, but is much subtler than in other tyrannosaurids. This is a potential autapomorphy of *Qianzhousaurus*, not recognized by Lü et al. (2014).

When in articulation with the other skull bones, the ventral process of the squamosal (Fig. 5) has a long axis oriented nearly anteroposteriorly, such that it approximately parallels the trend of the anterior process. This is a potential autapomorphy of *Qianzhousaurus*, not recognized by Lü et al. (2014), as the angle between the anterior and ventral processes is a more widely diverging, acute angle in *Alioramus altai* (Brusatte et al., 2012) and deep-snouted tyrannosaurids (e.g., Brochu, 2003; Currie, 2003; Hurum and Sabath, 2003). In *Qianzhousaurus*, the ventral process meets the quadratojugal to protrude deeply anteriorly into the lateral temporal fenestra, bisecting it into dorsal and ventral partitions. However, the squamosal-quadratojugal protrusion does not make contact with, or nearly touch, the postorbital-jugal bar that defines the anterior margin of the fenestra. This is also the case in *Alioramus altai* (Brusatte et al., 2012), but conversely, in some specimens of deep-snouted tyrannosaurids such as *Tyrannosaurus* (Osborn, 1912; Brochu, 2003) and *Gorgosaurus* (Currie, 2003), such contact occurs, or nearly does. In both *Qianzhousaurus* and *Alioramus altai* (Brusatte et al., 2012), the anterior end of the ventral ramus is squared off, a condition shared with deep-snouted tyrannosaurines such as *Tyrannosaurus* (Brochu, 2003), but differing from the tapered point of albertosaurines (e.g., Currie, 2003) and the tyrannosaurid outgroup *Bistahieversor* (Carr and Williamson, 2010).

The posterior process of the squamosal (Fig. 5) projects posteriorly from the region where the anterior and ventral processes meet. The lateral surface of the squamosal here is smoothly and deeply excavated by the lateral temporal fossa, much more so than in *Alioramus altai*, where the fossa is a pinched crescent (Brusatte et al., 2012), but more similar to the condition in deep-skulled tyrannosaurids (e.g., Brochu, 2003; Currie, 2003; Hurum and Sabath, 2003). The posterior process of *Qianzhousaurus* is a large, prominent, heel-like structure, which is rounded at its distal end. In size and dorsoventral orientation it is more similar to the large processes of deep-skulled tyrannosaurids such as *Daspletosaurus* (Currie, 2003), *Tarbosaurus* (Hurum and Sabath, 2003), and *Tyrannosaurus* (Brochu, 2003), although in these taxa the process is more square-shaped than distally rounded. *Alioramus altai* exhibits a strikingly different morphology, in which the posterior process, although broken on both sides of the holotype, is clearly much smaller, thinner, and sheet-like (Brusatte et al., 2012).

The squamosal is pneumatic. In ventral view, there is a large, funnel-like pneumatic opening that leads into an interior recess, the squamosal sinus (Witmer, 1997; Gold et al., 2013). This is also the case in most other tyrannosaurids (Carr and Williamson, 2010; Loewen et al., 2013; Brusatte and Carr, 2016:character 341). It is unclear, however, if the large pneumatic opening of *Qianzhousaurus* is associated with further, smaller pneumatic foramina. *Tyrannosaurus* has been described as having a single expansive opening (Brochu, 2003), but *Alioramus altai* has three smaller openings (Gold et al., 2013). The condition in *Qianzhousaurus* can probably only be determined via CT scanning, as in the aforementioned taxa. It is evident, however, that the internal squamosal sinus does not inflate the posterior process. This is also the case in *Alioramus altai*, *Teratophoneus*, and *Gorgosaurus*, whereas the sinus is more extensive and expands into the posterior process in *Daspletosaurus*, *Tarbosaurus*, and *Tyrannosaurus* (Brusatte and Carr, 2016:character 95).

Quadratojugal—The left quadratojugal is present and articulated within the skull (Figs. 1–5). As in other tyrannosaurids, this bone is L-shaped in lateral view, and is composed of two main processes: a dorsal process that expands dorsally to contact the ventral ramus of the squamosal to protrude into the lateral temporal fenestra, and an anterior process that is clasped by the jugal to form the ventral edge of the lateral temporal fenestra (Fig. 5).

The dorsal process (Fig. 5) is fan-shaped, and flares out dorsally to meet the squamosal, which it overlaps. The anterior margin of the lateral surface of the dorsal process is marked by a ridge, which is robust and extends to the dorsal margin of the bone, as in *Alioramus altai* (Brusatte et al., 2012), and most specimens of deep-snouted tyrannosaurines such as *Tyrannosaurus*, *Tarbosaurus*, and *Daspletosaurus* (Carr and Williamson, 2010; Brusatte et al., 2010; Brusatte and Carr, 2016:character 99). In contrast, *Albertosaurus* and *Gorgosaurus* have a fainter ridge that fades in strength dorsally. In *Qianzhousaurus*, the lateral surface of the dorsal process is deeply excavated by a smooth,

concave fossa (Fig. 5), similar to *Alioramus altai* (Brusatte et al., 2012) and other tyrannosaurids (e.g., Hurum and Sabath, 2003).

The anterior process is slender (Fig. 5), as in *Alioramus altai* (Brusatte et al., 2012), and differing from the much stouter, dorsoventrally deeper processes of deep-snouted tyrannosaurids (e.g., Brochu, 2003; Hurum and Sabath, 2003), and the close tyrannosaurid outgroup *Bistahieversor* (Carr and Williamson, 2010). The anterior tip of the anterior process is broken, but the suture on the lateral surface of the jugal gives an indication of its shape and extent. It projected slightly anterior to the anterior edge of the lateral temporal fenestra, as is normal for tyrannosaurids (see Brusatte et al., 2012), and it ended in a rounded tip, as in *Alioramus altai*, *Alioramus remotus*, albertosaurines (*Albertosaurus* and *Gorgosaurus*), not a deeper spatulate or squared tip as in the deep-snouted tyrannosaurines *Daspletosaurus*, *Tarbosaurus*, *Teratophoneus*, and *Tyrannosaurus* (Sereno et al., 2009; Carr and Williamson, 2010; Brusatte et al., 2010; Brusatte and Carr, 2016:character 101).

In posterior view, the medial surface of the quadratojugal (Fig. 7) is seen to make a broad contact with the quadrate (Fig. 7), which is interrupted by a large, teardrop-shaped quadrate foramen (Fig. 7), whose borders are nearly equally formed by the quadratojugal and quadrate. There is a deep fossa on the quadratojugal bordering the foramen laterally, and there is a small posterior tab on the quadratojugal (Fig. 8) that wraps around the quadrate posteriorly. In these features *Qianzhousaurus* is identical to *Alioramus altai*, and similar to tyrannosaurids generally (Brusatte et al., 2012).

Quadrate—The left quadrate is complete and well preserved (Fig. 1C, D), whereas the right quadrate (Fig. 1C, D) is broken and missing the condylar region. Because the left quadrate is preserved in articulation with the surrounding skull bones, it is best seen in posterior (Fig. 7) and ventral (Fig. 8) views.

Ventrally, the quadrate expands into two condyles, between which is the saddle-shaped articulation for the lower jaw. These are indistinguishable from the condyles of *Alioramus altai* (Brusatte et al., 2012) in that the entire condylar region is rectangular in ventral view, the medial condyle (Fig. 8) is slightly thicker anteroposteriorly, and the medial condyle projects further ventrally. Dorsal to the condylar region is the quadrate foramen (Fig. 7), described above, above which the quadrate forms a shaft that terminates in a rounded head, which is mostly obscured in posterior view.

In ventral view, two salient features of the quadrate are visible. First, there is a thin flange that projects anteriorly from the condylar region and shaft (Fig. 8). Most of the medial surface of the flange is freely exposed before it braces against the pterygoid at its anterior tip, and this medial margin is strongly concave, where it may have sat against an air sac (Currie, 2003), or perhaps provided muscle attachment. Second, at the corner where the anterior flange diverges from the condyles there is a deep, funnel-like opening that leads into the interior of the quadrate (Fig. 8). This is the external foramen for the quadrate recess, a pneumatic structure that fills the bone internally. This recess is present in *Alioramus altai* (Brusatte et al., 2012; Gold et al., 2013), and tyrannosaurids generally (e.g., Brusatte and Carr, 2016:character 106). Without CT data, however, we are unable to confirm the expanse of the recess inside the bone, or whether there were partitioned internal chambers inside the funnel-shaped opening like in *Alioramus altai*. It is clear, though, that there is no pneumatic foramen on the posterior surface of the quadrate shaft associated with the recess. Such a foramen is present in the basal tyrannosauroid *Dilong* and other coelurosaurs, but is absent in tyrannosaurids (Gold et al., 2013; Brusatte and Carr, 2016:character 318).

Palatine—Portions of the left and right palatine are present but broken (Fig. 9). They are best visible in ventral view, where they are in articulation on the skull midline, medial to the posterior end of the maxillary tooth row. Both left and right palatines can also be seen laterally through the window of the antorbital fenestra, but they are highly damaged; the left is slightly better preserved in this view. From what is preserved, the palatine appears highly similar to that of *Alioramus altai* (Brusatte et al., 2012).

In lateral view, it can be seen that the palatine has a maxillary process extending anteriorly to contact the medial surface of the maxilla and a jugal process posteriorly (Fig. 9B, C). Where these processes come together is the deeply indented, smooth surface of the internal antorbital fossa (Fig. 9), in the same position as in *Alioramus altai* (Brusatte et al., 2012). In *Alioramus altai*, this fossa leads into the window-like opening of the palatine recess posteriorly, which in turn expands into a pneumatic chamber that excavates much of the bone internally (Brusatte et al., 2012; Gold et al., 2013). Such pneumaticity characterizes tyrannosauroids generally (e.g., Brusatte and Carr, 2016:character 136), and although the details of the palatine recess are obscured by breakage and might require CT data to properly describe, palatine pneumaticity can confidently be inferred in *Qianzhousaurus*. Finally, above the antorbital fossa pneumatic region, the palatine fans out into a dorsal vomeropterygoid process (Fig. 9B, C), to contact the midline vomer, pterygoid, and opposing palatine; the size and shape of this process are not clear.

Some additional features of the palatine are apparent in ventral view. First, there is a fourth, medial process, which extends posteromedially to articulate with the pterygoid. The divergence of this process with the jugal process forms the suborbital fenestra in ventral view. Thus, the palatine of *Qianzhousaurus* is tetraradiate, as in *Alioramus altai* and tyrannosauroids generally. Also, although this region is highly damaged, it can be inferred that the suborbital fenestra was an anteroposteriorly elongate oval as in *Alioramus altai* and most tyrannosauroids, not circular as in the largest deep-skulled species such as *Tarbosaurus* and *Tyrannosaurus* (Brusatte et al., 2010; Brusatte and Carr, 2016:character 146). Similarly, the internal choana anteriorly (Fig. 9), between the vomeropterygoid and maxillary processes, would have been oval-shaped as in most tyrannosauroids and not circular as in the derived deep-skulled taxa (Brusatte et al., 2010; Brusatte and Carr, 2016:character 145). Finally, in *Qianzhousaurus*, the maxillary process is evidently elongate and thin, as in *Alioramus altai*, indicating that the palatine was anteroposteriorly elongate in concert with the external bones of the snout (maxilla and nasal). In contrast, the palatines of deep-snouted tyrannosaurids are anteroposteriorly short (e.g., Currie, 2003; Hurum and Sabath, 2003).

Pterygoid and Ectopterygoid—Portions of both bones are preserved on the right side of the skull, visible medial to the lacrimal-jugal contact (Fig. 3C, D). This part of the skull is so damaged, however, that these bones cannot be scored for phylogenetic characters (Brusatte and Carr, 2016), and all that can be said confidently is that the ectopterygoid makes broad contact with the jugal laterally.

Vomer—The anterior extent of the vomer is present and visible in ventral view, where it fits between the opposing maxillae on the midline (Fig. 2C, D). The vomer is clearly anteroposteriorly elongate, in concert with the elongate palatine, maxilla, and nasal, and together these bones define the stretched snout region. The vomer is lanceolate in shape and expands ever so slightly laterally on both sides towards its anterior margin, as in tyrannosauroids generally, but it does not expand into the greatly enlarged anterior diamond of *Tarbosaurus* (Hurum and Sabath, 2003) and *Tyrannosaurus* (Brochu, 2003; Sereno et al., 2009; Brusatte et al., 2010; Carr and Williamson, 2010; Brusatte and Carr, 2016:character 128).

Mandible

The right mandible is preserved with the jaw bones in articulation, but part of its middle section is missing (Fig. 10). Thus, portions of the dentary, surangular, angular, prearticular, and

splenial have been lost. The genuine anterior and posterior sections of the mandible were joined during conservation of the specimen, and the missing region is now filled in with artificial material in its current condition in the Ganzhou Museum. The shape of the resulting mandible is reasonably accurate, but slightly too deep dorsoventrally in the reconstructed missing region. Also note that this break obscures the details of the external mandibular fenestra.

Dentary—The dentary is almost complete and well preserved (Figs. 10, 11). Similar to the morphology of the snout, the dentary is also gracile, elongate, and shallow as in *Alioramus altai* (Brusatte et al., 2009, 2012). This differs from the deeper and stouter dentaries of large, deep-skulled tyrannosaurids (e.g., Brochu, 2003; Currie, 2003; Hurum and Sabath, 2003).

The general outline of the dentary is consistent with that of other tyrannosaurids, both long-snouted and deep-skulled forms, in that it is dorsoventrally deepest posteriorly where it meets the surangular, then shallows along the tooth row, before expanding somewhat at its anterior tip. With that said, *Qianzhousaurus* is different from all other tyrannosaurids, including the long-snouted *Alioramus altai* (Brusatte et al., 2009, 2012) and deep-snouted species such as *Tyrannosaurus* (Brochu, 2003) and *Gorgosaurus* (Currie, 2003), in one notable way: there is no projecting 'chin' at the anteroventral corner of the dentary (Brusatte et al., 2010; Brusatte and Carr, 2016:character 172). The 'chin' is present as a discrete bump that extends from the corner of the dentary in deep-snouted species, and expressed as more of a low convexity that braces the dentary symphysis in *Alioramus altai*. In *Qianzhousaurus*, however, the anterior edge of the dentary smoothly merges with the ventral margin, along a rounded curve. This is an autapomorphy of *Qianzhousaurus* among tyrannosaurids, noted in the description of Lü et al. (2014) but not listed as part of the diagnosis of *Qianzhousaurus*.

In lateral view, the dorsal margin of the dentary along the tooth row is concave, as in other tyrannosaurids. The ventral margin is straight to slightly convex anteriorly, and then posteriorly becomes more strongly convex as the dentary fans out in depth. This is similar to deep-snouted tyrannosaurids such as *Tyrannosaurus* (Brochu, 2003), *Tarbosaurus* (Hurum and Sabath, 2003), *Lythronax* (Loewen et al., 2013), and *Gorgosaurus* (Currie, 2003), but differs from *Alioramus altai*, wherein the ventral margin of the dentary is nearly straight across its entire length, only expanding ever so slightly at its posterior end (Brusatte et al., 2009, 2012). Finally, the anterior margin of the dentary in *Qianzhousaurus* is gently angled at ~45° relative to the long axis of the bone, as in *Alioramus altai* (Brusatte et al., 2012) and albertosaurines (Currie, 2003), but unlike the much steeper margin of many tyrannosaurines, which is oriented at approximately a right angle to the dentary axis (Carr and Williamson, 2010; Loewen et al., 2013; Brusatte and Carr, 2016: character 358). This latter condition is present, for example, in *Lythronax* (Loewen et al., 2013), *Zhuchengtyrannus* (Hone et al., 2011), *Tarbosaurus* (Hurum and Sabath, 2003), and *Tyrannosaurus* (Brochu, 2003).

In dorsal view, the tooth row of *Qianzhousaurus* is wide, with a convex lateral surface. Posterior to the alveoli, the dentary noticeably thins into a plate-like region, before making contact with the surangular, which overlaps the dentary laterally in this area.

The lateral surface of the dentary is rugose as in other tyrannosaurids. Two rows of neurovascular foramina run largely parallel to each other (Fig. 10). The first is positioned ventral to the alveolar margin of the dentary tooth row and follows the concave trajectory of the dorsal dentary margin. The first row is closer to the dorsal margin of the dentary anteriorly, and then sweeps ventrally as it continues posteriorly. Individual foramina are more distinct as individual round openings, and are greater in number anteriorly, and they become sparser posteriorly, anterior to an open groove located at the back of the tooth row. The groove continues onto the lateral surface of the surangular. In these respects, the dorsal row of foramina is very similar to that in *Alioramus altai* (Brusatte et al., 2012). The second row of foramina in *Qianzhousaurus* is located immediately above the ventral margin of the dentary and follows the straight contour of the bone, before dissipating posteriorly where the dentary expands dorsoventrally. As in the dorsal row, these foramina are better defined anteriorly, and become sparser and more anteroposteriorly elongate posteriorly. Furthermore, as in other tyrannosaurids, there is a cluster of several randomly arrayed foramina at the anterior end of the dentary, between the dorsal and ventral foramina rows.

In medial view, the articulated supradentary/coronoid (Fig. 10) obscures the alveoli and interdental plates of the dentary. Ventrally, however, the medial surface of the dentary is exposed and well preserved. Anteriorly, the symphyseal surface for the opposing dentary is generally smooth (Fig. 11), with some rugosities ventrally that parallel the anterior margin of the bone. This is similar to the condition in *Alioramus altai* (Brusatte et al., 2012), albeit the symphysis is slightly more rugose in *Qianzhousaurus*. In contrast, derived deep-snouted tyrannosaurines such as *Tarbosaurus* (Hurum and Sabath, 2003), *Tyrannosaurus* (Brochu, 2003), *Daspletosaurus* (Currie, 2003), and *Zhuchengtyrannus* (Hone et al., 2011) have much more strongly rugose symphyseal surfaces, which are bevelled and scoured with interlocking ridges and convexities for articulation with the opposing symphysis (Brusatte et al., 2010; Brusatte and Carr, 2016:character 173).

The other salient feature of the medial surface is the Meckelian groove (Fig. 11), which follows the long axis of the dentary across approximately the mid-depth of the bone. It is similar in morphology to that of *Alioramus altai* (Brusatte et al., 2012), in that it is sharp anteriorly (dorsoventrally thin and deeply incised into the bone) but posteriorly funnels out into a shallower fossa (Fig. 12), which then becomes overlapped by the splenial (Fig. 12). At its anterior tip, the groove terminates in a small anterior Meckelian foramen (Fig. 11). The position of the foramen, in the vicinity of alveoli five and six, is similar to that in *Alioramus altai* and tyrannosaurids generally (Brusatte et al., 2012). Finally, as seen in medial view (Fig. 12), the articular surface for the splenial along the ventral region of the dentary ramus below the Meckelian groove (and then fossa) is dorsoventrally shallow and smooth, as in *Alioramus altai* and albertosaurines, not so deep that it is nearly as deep as the anterior region of the fossa itself, as is the case in derived deep-snouted tyrannosaurines such as *Tarbosaurus*, *Tyrannosaurus*, *Daspletosaurus*, and *Zhuchengtyrannus* (Brusatte et al., 2010; Brusatte and Carr, 2016:character 174).

There are 18 dentary alveoli in *Qianzhousaurus*. This is the same number as in the holotype of *Alioramus remotus* (Kurzanov, 1976), but less than the 20 in the holotype of *Alioramus altai* (Brusatte et al., 2009, 2012). All three of these long-snouted alioramins, however, exhibit a noticeably greater tooth count than deep-snouted tyrannosaurids: *Tyrannosaurus* possesses 12–17 dentary teeth depending on ontogenetic stage (tooth loss occurred through ontogeny: Carr, 1999, 2020; Carr and Williamson, 2004), and no non-alioramin tyrannosaurid specimen, to our knowledge, has more than 17 dentary teeth. Thus, all three alioramins are united by the derived condition of 18 or more dentary teeth, as encapsulated in the phylogenetic character of Lü et al. (2014:character 317) and Brusatte and Carr (2016:character 315).

In *Qianzhousaurus*, the first two alveoli are markedly smaller than those in the midpoint of the tooth row. This is also the case in *Alioramus altai*, *Daspletosaurus*, and albertosaurines, but contrasting with the condition in *Tarbosaurus* and *Tyrannosaurus*, in which only the first alveolus is abnormally small (Brusatte et al., 2010; Brusatte and Carr, 2016:character 175). Execpt for those

at the very front and back of the tooth row, the alveoli of *Qianzhousaurus* are rectangular in shape, but with rounded corners as seen in dorsal view. This is somewhat similar to *Alioramus altai*, although its alveoli are more square-shaped, with sharper corners, and many are pinched in the middle, giving them more of a figure-8 profile (Brusatte et al., 2012). These, like the maxillary alveoli, imply that the dentary teeth were incrassate in shape. As with the maxilla, all erupted teeth from the dentary are missing.

Surangular—The anterior and posterior regions of the right surangular are present, but the bone is missing its middle portion (Fig. 13). In overall shape, the surangular of *Qianzhousaurus* is anteroposteriorly elongate and dorsoventrally shallow, as in *Alioramus altai* (Brusatte et al., 2012). Adult deep-snouted tyrannosaurids, on the other hand, have a shorter and deeper surangular (e.g., Hurum and Currie, 2000; Brochu, 2003; Currie, 2003; Hurum and Sabath, 2003; Loewen et al., 2013). Thus, the long and gracile skull shape of *Qianzhousaurus* (and *Alioramus*) manifests itself in the posterior part of the lower jaw, despite the fact that the posterior part of the upper skull (jugal, postorbital, quadratojugal, squamosal) is not elongated anteroposteriorly.

The surangular is thickened dorsally; but is a mediolaterally thin plate ventrally. Its lateral surface (Fig. 13A) is smooth where it overlaps the dentary. Most of this contact is preserved, although a portion of it is missing posteriorly. There is a large gap between the two bones at this articulation, filled with sediment, which suggests that the joint would have allowed a degree of motion in life, as in *Alioramus altai*.

Anteriorly a long, tapering process of the surangular is seen to slot into the dentary when the two bones are in articulation, as in *Alioramus altai* (Brusatte et al., 2012:fig. 4). This process is short in large deep-snouted tyrannosaurids such as *Gorgosaurus* (Currie, 2003:fig. 2), *Tyrannosaurus* (Hurum and Currie, 2003: fig. 2; Brochu, 2003:fig. 40), *Daspletosaurus* (Currie, 2003:fig. 36), *Lythronax* (Loewen et al., 2013:fig. 2), and *Teratophoneus* (Loewen et al., 2013:fig. 3). This is related to, but not identical with, a phylogenetic character encapsulating the elongate proportions of the surangular that unites *Qianzhousaurus* and *Alioramus* into Alioramini: the length of the anterior flange (the region of the surangular anterior to the anterior margin of the external mandibular fenestra) is greater than 30% of the overall length of the bone (Brusatte et al., 2010; Brusatte and Carr, 2016:character 187). Thus, the finger-like process may be a synapomorphy of alioramins, in addition to characters relating to the overall proportions of the surangular.

The dorsal edge of the surangular is a laterally projecting surangular shelf (Fig. 13). The shelf is prominent and dorsoventrally deep as in all tyrannosaurids (Sereno et al., 2009; Carr and Williamson, 2010; Brusatte et al., 2010; Brusatte and Carr, 2016:character 180), and also extends approximately straight anteroposteriorly in line with the long axis of the surangular as in other tyrannosaurids (Brusatte et al., 2010; Brusatte and Carr, 2016:character 182). Above the shelf is a deep attachment site for the jaw adductor muscles (Fig. 14). This surface faces almost equally dorsally and laterally, as in *Alioramus altai*, albertosaurines, and *Teratophoneus* (Brusatte et al., 2010; Brusatte and Carr, 2016:character 184). In contrast, the largest deep-snouted forms such as *Lythronax*, *Tarbosaurus*, *Tyrannosaurus*, and some specimens of *Daspletosaurus* have a muscle attachment that is so deep that it takes the form of a flange dorsal to the ridge, with a muscle attachment surface nearly entirely laterally facing. Unfortunately, the surface preservation of the surangular shelf and adjoining regions in *Qianzhousaurus* is too poor to determine whether it possessed the series of small fossae that are phylogenetically informative in tyrannosauroids generally (Brusatte et al., 2010, 2012; Brusatte and Carr, 2016:characters 185–186).

In *Qianzhousaurus*, there is an expansive surangular foramen ventral to a surangular shelf (Fig. 13). As in other tyrannosaurids, the foramen is so large that it takes the form of a fenestra, ~30% of the depth of the entire posterior half of the surangular (Sereno et al., 2009; Carr and Williamson, 2010; Brusatte et al., 2010; Brusatte and Carr, 2016:character 179). The surangular foramen abuts the surangular shelf dorsally, and the shelf projects laterally here, as in *Alioramus altai* and albertosaurines. In contrast, the shelf is tilted ventrolaterally to overhang the foramen in large deep-snouted tyrannosaurines such as *Tarbosaurus*, *Tyrannosaurus*, *Daspletosaurus*, *Teratophoneus*, and *Lythronax* (Brusatte et al., 2010; Carr and Williamson, 2010; Brusatte and Carr, 2016:character 181). In *Qianzhousaurus* there is a deeply incised pneumatic pocket posterodorsal to the surangular foramen (Fig. 13), as in tyrannosaurids broadly (Brusatte et al., 2010; Gold et al., 2013; Brusatte and Carr, 2016:character 183). Further details of pneumaticity in this region, including whether there is a chamber inside the surangular, await confirmation from CT scanning, as Gold et al. (2013) did for *Alioramus altai*.

The surangular contacts several lower jaw bones in addition to the dentary. At the posteroventral corner of the jaw it articulates with the angular (Fig. 10). It appears as if the angular overlaps the surangular here in lateral view, as in *Alioramus altai* (Brusatte et al., 2012). The splenial, prearticular, and supradentary/coronoid (Fig. 10) all make contact with the medial surface of the anterodorsal region of the surangular, but again the articulated nature of the jaw makes describing the details challenging. The articular, likely along with a small portion of the prearticular, latches against the medial surface of the posterior part of the surangular, at the retroarticular process. In dorsal view, the anterolateral region of the glenoid fossa for articulation with the quadrate of the upper skull is on the surangular (Fig. 14). The posteromedial part of the glenoid is on the articular; the surangular and articular components each make up approximately half of the glenoid joint.

The retroarticular process of the surangular, which extends posteriorly beyond the glenoid as a flange (Figs. 13–14), is anteroposteriorly short as in tyrannosauroids (e.g., Holtz, 2001; Brusatte et al., 2014). It is triangular in shape, with a posteroventrally sloping posterior margin, similar to *Alioramus altai* (Brusatte et al., 2012) but differing from the more vertical posterior margin of deep-skulled tyrannosaurids, such as *Gorgosaurus* (Carr, 1999; Currie, 2003), *Daspletosaurus* (Carr, 1999), *Tarbosaurus* (Hurum and Sabath, 2003), *Tyrannosaurus* (Brochu, 2003), and *Lythronax* and *Teratophoneus* (Loewen et al., 2013). This distinction has not been encapsulated into a phylogenetic character in previous tyrannosauroid datasets, but the posteroventral condition may be a synapmorphy of alioramins. It is, however, also present in some juveniles of deep-skulled species like *Gorgosaurus* (Carr, 1999), so its phylogenetic utility may be problematic.

Angular—The right angular is mostly intact, but is missing its anterior end (Fig. 10). The bone consists of two processes: a shallow anterior process (some of which is missing) and a deeper, plate-like posterior process, that likely overlaps the surangular. The ventral margin of the bone is smoothly convex where these processes meet, as in *Alioramus altai* (Brusatte et al., 2012), albertosaurines (Currie, 2003), and close tyrannosaurid outgroups such as *Bistahieversor* (Carr and Williamson, 2010). In contrast, deep-skulled tyrannosaurines such as *Tyrannosaurus* (Brochu, 2003), *Tarbosaurus* (Hurum and Sabath, 2003), and *Teratophoneus* (Loewen et al., 2013) have a kinked angular, wherein the anterior region is flexed relative to the posterior region, such that there is a discrete step between them (Brusatte and Carr, 2016:character 188; Brusatte et al., 2010). Details of the contacts with the prearticular, splenial, and possibly the articular are obscured by the articulation between the bones.

Articular—The right articular (Fig. 14) is preserved in firm articulation with the surangular laterally and prearticular medially, and apparently were tightly joined in life permitting very

little motion between them. The dorsal surface of the articular is visible, and several key details of the glenoid and retroarticular process are apparent. Given that the articular is not currently known and described for *Alioramus* (Brusatte et al., 2012), *Qianzhousaurus* therefore provides the first information on the details of this bone in a long-snouted alioramin.

In *Qianzhousaurus*, the articular forms the posteromedial half of the smooth glenoid joint for the quadrate with surangular comprising the anterolateral half. The retroarticular process of the articular is short, as in tyrannosauroids generally, and consistent with the adjacent short retroarticular process of the surangular, described above. The joint surface of the glenoid (Fig. 14) essentially abuts the concave jaw muscle attachment site on the dorsal surface of the retroarticular process, with only a thin ridge between them. This is similar to other tyrannosaurids, but differs from the condition in the most basal tyrannosauroids and other theropods, in which there is a wide, smooth, non-articular surface between the glenoid and muscle attachment fossa (Brusatte et al., 2010; Rauhut et al., 2010; Brusatte and Carr, 2016:character 190). Furthermore, the mediolateral width of the muscle attachment is greater than the width of the glenoid, another feature shared with other tyrannosaurids but contrasting with the mediolaterally narrow muscle fossa in the most basal tyrannosauroids and other theropods (Brusatte et al., 2010; Rauhut et al., 2010; Brusatte and Carr, 2016:character 189).

The jaw muscle attachment fossa on the retroarticular process faces posterodorsally in *Qianzhousaurus*. This is consistent with the posteroventrally sloping posterior margin of the retroarticular process of the surangular in lateral view. This suite of characters, as noted above, may characterize alioramins, as deep-skulled tyrannosaurids have more vertical posterior edges of the retroarticular process, and thus more strictly posteriorly facing jaw muscle attachment sites on the articular. At present, however, it is unclear if this variation relates to ontogeny or phylogeny.

Prearticular—Much of the right prearticular is present on the articulated lower jaw, although the middle portion is missing (Fig. 10). As in other tyrannosaurids, the prearticular is a mediolaterally thin and arched bar of bone that spans across most of the medial surface of the surangular, and is widely visible when the jaw is observed in medial view. Anteriorly the prearticular expands into a spade-shaped anterior process, and posteriorly into a medially convex cup that embraces the articular. In between these two processes is a bar of bone; that is the shallowest part of the prearticular. The overall shape of the prearticular is somewhat intermediate between the elongate and shallowly curved profile of *Alioramus altai* (Brusatte et al., 2012) and the much more deeply arched shape of adult deep-snouted tyrannosaurids such as *Tyrannosaurus* (Brochu, 2003) and *Tarbosaurus* (Hurum and Sabath, 2003). Curvature of the bone is known to increase during tyrannosaurid ontogeny (Carr, 1999), in concert with the deepening of the jaw, so the phylogenetic utility of this feature is uncertain.

The medial surface of the prearticular is generally smooth. There appears to be an ovoid foramen (Fig. 10), filled with sediment, towards the anterior end of the anterior process. However, we are unable to confirm whether this is genuine (in which case it would be an autapomorphy of *Qianzhousaurus* among tyrannosaurids), or an artifact of taphonomic or preparation damage.

The anterior process is strap like, and tapers anteriorly at a low angle. This is similar to the condition in *Alioramus altai* (Brusatte et al., 2012), but contrasts with the deeper, more wedge-shaped anterior processes of adult deep-snouted tyrannosaurids.

The anterior process has complex articulations with surrounding lower jaw bones, as it contacts the surangular, splenial, and supradentary/coronoid, but apparently not the dentary. In medial view, the anterior margin of the anterior process appears to abut the splenial, but in fact the splenial medially overlaps a small portion of the prearticular here, as in *Alioramus altai* (Brusatte et al., 2012) and deep-snouted tyrannosaurids such as *Tarbosaurus* and *Tyrannosaurus* (Hurum and Currie, 2000; Brochu, 2003; Hurum and Sabath, 2003). Posterior to this contact, the splenial and prearticular are separated from each other by a small foramen/fenestra, but contact once more near the ventral margin of the mandible, at a simple abutting suture where the ventral edge of the prearticular sits atop the dorsal edge of the splenial. No contact between these bones is shown in this position in the reconstructed articulated lower jaws of *Tarbosaurus* and *Tyrannosaurus* (Hurum and Currie, 2000; Brochu, 2003; Hurum and Sabath, 2003); instead, the gap between the prearticular and splenial is wider, and extends to the ventral margin of the dentary, exposing the angular in medial view here. Poor preservation and breakage in most specimens make interpreting these discrete features difficult, however. The condition in *Alioramus altai* is not immediately clear, as the bones are not preserved in articulation, yet it has a convex notch on the ventral margin of its prearticular anterior process in the same position where a convexity on the prearticular makes contact with the splenial in *Qianzhousaurus*, suggesting that it shared the same morphology (Brusatte et al., 2012). Because articulated lower jaws are rare among tyrannosauroids, it is not yet clear whether alioramins share a derived morphology, or whether deep-skulled tyrannosaurids share a derived morphology, or whether this is random variation.

Further posteriorly, the prearticular makes contact with several other bones of the mandible. The bar-shaped central part of the prearticular contacts the angular laterally. Details of this joint surface are obscured by the articulated condition of the jaw bones, and breakage in this region. It is clear, however, that the ventral margin of the central bar (and the adjacent posterior process) is smooth, and lacks the rugosities of *Tyrannosaurus* (Brochu, 2003). The posterior process expands into a triangular shape in medial view. It clearly contacts both the articular and surangular, and almost certainly cupped the articular across most of its depth, with slightly made contact with the surangular dorsally and ventrally (based on comparisons to *Alioramus altai*; Brusatte et al., 2012). The degree of fusion between the bones of the prearticular and the bones of the posterior mandible is difficult to decipher, given the articulation of the jaw and the remaining matrix. Parts of the prearticular, angular, articular, and surangular are fused here in large individuals of *Tarbosaurus* (Hurum and Currie, 2000; Hurum and Sabath, 2003), but there is no fusion in *Alioramus altai* (Brusatte et al., 2012).

Articulation between the prearticular and articular occurs on the posterior face of the posterior process of the prearticular at a cup-like contact that grips the articular on its ventral face. Although the lateral surface of the prearticular is obscured, there appears to be at least some fusion between the posterior process of the prearticular with the articular and surangular, unlike in *A. altai* which sees no fusion with the surangular and only light articulation with the articular. The condition in *Qianzhousaurus* is closer in similarity with that of *Tyrannosaurus* and *Tarbosaurus*, which exhibit a similarly fused condition.

Splenial—The right splenial (Figs. 10, 11) is preserved in articulation with the surrounding jaw bones, and it is nearly complete, and only the posterior tip of the posterior process has been lost. As in all tyrannosaurids, the splenial covers much of the medial surface of the posterior dentary in medial view, and is roughly triangular and composed of three main processes: an anterior process that extends nearly straight anteriorly following the long axis of the jaw, a posteroventrally descending posterior process, and a dorsal flange (Fig. 12). The posterior process and dorsal flange diverge from each other at an acute angle in medial view, as in *Alioramus altai* (Brusatte et al., 2012). This angle is more obtuse, and thus the two processes separate more widely

from each other, in large deep-snouted tyrannosaurids such as *Tyrannosaurus* (Brochu, 2003) and *Tarbosaurus* (Hurum and Sabath, 2003), in concert with the mediolaterally deeper jaws of these species. The shallower divergence of the processes in *Alioramus altai*, which manifests itself as a dorsal flange with a more horizontal long axis compared with the more anteroventral axis of deep-snouted species, was considered a possible autapomorphy of *Alioramus altai* by Brusatte et al. (2012). Given its occurrence in *Qianzhousaurus*, this suggests the character is an alioramin synapomorphy.

The anterior process is long and triangular, and is separated from the dorsal flange by a small notch, as in *Alioramus altai* (Brusatte et al., 2012), and other tyrannosaurids (e.g., Brochu, 2003). The anterior process covers the medial surface of the Meckelian groove (Fig. 11) and fossa (Fig. 12) on the dentary. The dorsal flange has a long, nearly straight, gently sloping anterior margin and a shorter, more steeply sloping posterior edge. It contacts both the dentary and the supradentary/coronoid laterally. The dorsal flange slightly overlaps the prearticular medially, as in *Alioramus altai* (Brusatte et al., 2012), whereas it is the prearticular that overlaps the splenial here in *Daspletosaurus*, *Tarbosaurus*, and *Tyrannosaurus* (Brusatte et al., 2010; Brusatte and Carr, 2016:character 192). This latter condition is well illustrated in *Tyrannosaurus* by Brochu (2003:fig. 40) and *Tarbosaurus* (Hurum and Sabath, 2003:fig. 20). The posterior process tapers posteriorly. It is separated from the dorsal flange by a notch, which is much larger and more open than the notch between the anterior process and dorsal flange. Compared with *Alioramus altai* (Brusatte et al., 2012), the notch is slightly more widely open, and more rounded. With the lower jaw bones in articulation, this notch forms the open space between the splenial and the anterior process of the prearticular.

The anterior mylohyoid foramen pierces the anterior process of the splenial. It is expressed as an anteroposteriorly elongate oval, similar to that of *Alioramus altai* (Brusatte et al., 2012), although slightly deeper dorsoventrally. The anteroposteriorly elongate foramen was previously considered autapomorphic of *Alioramus altai* (Brusatte et al., 2009, 2012), but is now known to be present in *Qianzhousaurus*, and is thus an alioramin synapomorphy. In contrast, deep-skulled tyrannosaurids such as *Daspletosaurus* (Currie, 2003), *Tyrannosaurus* (Brochu, 2003) and *Tarbosaurus* (Hurum and Sabath, 2003) have much larger, more circular foramina that are nearly as deep dorsoventrally as the entire anterior process (Brusatte et al., 2010; Carr and Williamson, 2010; Brusatte and Carr, 2016:character 191).

In *Qianzhousaurus*, the anterior mylohyoid foramen is entirely enclosed within the splenial (Fig. 12) as in *Alioramus altai* (Brusatte et al., 2012) and most tyrannosaurid specimens, but it does breach the ventral margin of the bone in most deep-snouted tyrannosauroids. The foramen is positioned higher from the ventral margin of the splenial in the *Qianzhousaurus* holotype, compared with the *Alioramus altai* holotype, supporting the hypothesis that the foramen became more enclosed within the splenial during ontogeny (Currie and Zhiming, 2001). Slightly anterior and posterior to the anterior mylohyoid foramen in *Qianzhousaurus* is an accessory fossa depression (Fig. 10), as also described in *Alioramus altai* (Brusatte et al., 2012).

Supradentary/Coronoid—The right supradentary/coronoid (Fig. 10) is present and is well preserved, in articulation with the dentary, splenial, and prearticular. Although the details of these contacts are not easily observable due to the articulated nature of the specimen. The anterior supradentary and posterior coronoid portions are firmly fused into one element. These two portions are confluent as in *Alioramus altai* (Brusatte et al., 2012) and *Daspletosaurus* (Currie, 2003), unlike *Tyrannosaurus* (Brochu, 2003) and *Tarbosaurus* (Hurum and Sabath, 2003), in which they are offset by a concave notch (Brusatte et al., 2010; Brusatte and Carr, 2016:character 195).

The supradentary region follows the contours of the tooth row, covering it (and the interdental plates of the dentary) medially. The supradentary is an elongate, shallow strip like in *Alioramus altai* (Brusatte et al., 2012) and most tyrannosauroids, but not a deep, crescentic bone as in *Tyrannosaurus* (Brochu, 2003) and *Tarbosaurus* (Hurum and Sabath, 2003) (Brusatte et al., 2010; Brusatte and Carr, 2016:character 194). The dorsal margin of the supradentary is much more concave in *Qianzhousaurus* than in *Alioramus altai* (Brusatte et al., 2012) and deep-snouted *Daspletosaurus* (Currie, 2003), *Tyrannosaurus* (Brochu, 2003), and *Tarbosaurus* (Hurum and Sabath, 2003); this is potentially an autapomorphy of *Qianzhousaurus* among tyrannosaurids.

The coronoid region of *Qianzhousaurus* is much smaller than the supradentary, and triangular in shape. Only portions of this region are visible in the articulated jaw, with many cracks in this region making it difficult to distinguish sutures from breakage. Very little of the coronoid is observable on the specimen in medial view, compared with the condition in *Tyrannosaurus* (Brochu, 2003) and *Tarbosaurus* (Hurum and Sabath, 2003), where it is visible along the dorsal margin of the jaw posterior to the prearticular. If genuine, the limited medial exposure of the coronoid may be autapomorphic among tyrannosaurids, with the caveat that the condition in *Alioramus altai* is uncertain because the jaw bones were found loose and not in articulation (Brusatte et al., 2012). Alternatively, it may actually be that a large portion of the coronoid is visible here, taking the form of an anteroposteriorly elongate triangular shape (Fig. 10), which projects far posterior to the prearticular. If this is the case, then the elongate coronoid, which is widely visible in medial view when the jaws are articulated, would be autapomorphic of *Qianzhousaurus*.

DISCUSSION

Qianzhousaurus Autapomorphies

In their short initial paper describing the *Qianzhousaurus* type specimen, Lü et al. (2014) identified two autapomorphic characters in the crania. These distinguished *Qianzhousaurus* from the long-snouted *Alioramus* and other, more traditional deep-snouted tyrannosaurids. They were: an extremely reduced premaxilla with an anteroposterior length of less than 2.2% of basal skull length and a window-like pneumatic fenestra (Fig. 1A, B) in the ascending ramus of the maxilla, anterior to the antorbital fenestra, which is present on both sides of the skull. Our more detailed description and comparisons confirm that both features are currently unique among tyrannosaurids, and thus autapomorphic of *Qianzhousaurus*. We do note, however, that because the premaxilla is currently unknown in all described specimens of *Alioramus*, the particularly tiny premaxilla may turn out to be a synapomorphy of Alioramini (*Alioramus* + *Qianzhousaurus*).

Our more through description of the *Qianzhousaurus* holotype cranium, and more comprehensive comparisons with other tyrannosaurids, reveals several new possible autapomorphies, some of which are currently equivocal due to preservation and post-collection damage to the bones. These new autapomorphies are: a fused nasal element that is rod-like in dorsal view and does not expand laterally around the bony naris (instead of a more hourglass-shape, although straight lateral margins are also seen in *Gorgosaurus* Carr, 1999, there is still considerably lateral convexity around the bony naris region), a ventral process of the lacrimal oriented anteroventrally (instead of more vertically in other tyrannosaurids), a gracile and shallow dorsal prong of the anterior ramus of the squamosal (lacking a deep flange extending dorsal to the main body of the process; we note that the gracile and shallow condition may also be

present in *Alioramus remotus*; Kurzanov, 1976), a ventral process of the squamosal oriented anteroposteriorly (nearly paralleling the anterior process of the bone, instead of diverging widely at an acute angle), a dentary in which the anterior edge smoothly merges with the ventral margin along a curve (with no projecting dentary 'chin'), and a supradentary with a highly concave dorsal margin.

We also note two characters that could potentially be autapomorphies of *Qianzhousaurus*, but are highly equivocal. First, an ovoid foramen on the medial surface of the prearticular, which is uncertain due to poor preservation and infilling sediment, and the fact that there is no surrounding fossa (which would be supporting evidence that it is a real opening). Careful study of the prearticular, likely under microscopic scrutiny, may be required to confirm whether this feature is a genuine foramen, a pathological lesion, or postmortem damage to the specimen. Second, limited medial exposure of the coronoid when the lower jaw is seen in articulation in medial view. This is uncertain due to the difficulty of distinguishing sutures between the articulated bones. Indeed, alternatively, if we have not been able to distinguish the sutures correctly, it may be that the coronoid is actually extremely elongated and broadly visible in articulation in medial view, which could also be an autapomorphy.

In total, these additional autapomorphies increase the morphological divergence between *Qianzhousaurus* and *Alioramus*, further supporting the former as a distinct genus from the latter. However, as the holotype of *Qianzhousaurus* is more mature than any described *Alioramus* specimen, including the holotypes of *Alioramus remotus* (Kurzanov, 1976) and *Alioramus altai* (Brusatte et al., 2009, 2012), it may be that some of these putative autapomorphies are ontogenetically controlled, and thus would not be supportive of taxonomic separation. Only further discovery and description of ontogenetic series of alioramins can help clarify this issue.

Alioramini Synapomorphies

In their initial description of *Qianzhousaurus*, Lü et al. (2014) named the clade Alioramini as a subclade of Tyrannosaurinae, to incorporate the long-snouted *Qianzhousaurus* and both species of *Alioramus*. This clade was supported by several synapomorphies shared by *Qianzhousaurus* and at least one of the *Alioramus* species (many features in *Alioramus remotus* are uncertain due to missing data). These include: a longirostrine skull morphology in which the snout occupies 2/3 of the total skull length; an anteroposteriorly elongate maxillary fenestra (ratio of maximum anteroposterior length to maximum dorsoventral depth greater than 1.9); a series of discrete, pronounced rugosities on the dorsal surface of the nasals; and 18 or more dental alveoli/teeth. These characters were included in the phylogenetic analyses of Brusatte and Carr (2016) and Carr et al. (2017), and optimized as alioramin synapomorphies. Our more thorough description of the *Qianzhousaurus* holotype and comparison with other tyrannosaurids reiterates that these features are currently only known in alioramins among tyrannosaurids.

We here note additional features that may be synapomorphic for Alioramini, as they are present in *Alioramus* and *Qianzhousaurus*. They should be included in future phylogenetic analyses of tyrannosauroids. First, a laterally projecting rugosity on the jugal, above the cornual process, which takes the form of a well-defined horn in *Alioramus* and more of a swollen ridge in *Qianzhousaurus*. Although the shape of the structure differs in these two alioramins, it is likely homologous, as laterally extending rugosities are absent in all other tyrannosaurids. Second, a long, tapering, finger-like process of the surangular that extends anteriorly to slot into the dentary when the two bones are in articulation. This is seen in *Alioramus*, but absent in deep-snouted species such as *Tyrannosaurus*, although it may be at least partially related to an existing phylogenetic character that encapsulates the overall length of the anterior flange of the surangular (Brusatte and Carr, 2016:character 187). Third, a splenial in which the posterior process and dorsal flange diverge from each other at an acute angle (as opposed to the more obtuse angle, which separates the processes more widely, in large deep-snouted and deep-jawed tyrannosaurids such as *Tyrannosaurus* and *Tarbosaurus*). As part of this condition, the dorsal flange of alioramins has a more horizontal long axis compared with the more anteroventral axis of deep-snouted tyrannosaurids. This was considered a possible autapomorphy of *Alioramus altai* by Brusatte et al. (2012), but here is revealed as shared with *Qianzhousaurus*, and thus an alioramin synapomorphy (although it may be partially related to ontogeny, as it is related to the overall depth of the mandible). Fourth, an anterior mylohyoid foramen on the splenial shaped like an anteroposteriorly elongate oval, compared with the larger circular foramina of deep-snouted tyrannosaurids. This was considered an autapomorphy of *Alioramus altai* by Brusatte et al. (2009, 2012), but is now synapomorphic of *Alioramus* + *Qianzhousaurus*. It should be noted that the third and fourth points above are likely related to the general shallowing of the alioramin skull, and thus are part of a package of synapomorphies ultimately related to overall skull shape.

Alioramin Skull Shape

Our observations and comparisons clarify the nature of the elongated skull that is unique to alioramins among tyrannosaurids. In describing *Alioramus altai*, Brusatte et al. (2012:11) considered the long skull shape to be 'mostly a function of elongated snout bones, anterior to the orbit, including the maxilla, nasal, jugal, lacrimal, and dentary,' and they explicitly referred to it as a 'longirostrine' skull. Lü et al. (2014:2), in their initial description of *Qianzhousaurus*, concurred, stating that 'the individual bones of the snout such as the maxilla and nasal are elongated, whereas those of the posterior skull are of similar proportions to other large tyrannosaurids.' Furthermore, in describing the first premaxilla for an alioramin, they noted that this bone at the front of the snout was not elongated, lengthened, or modified in any substantial way.

We here add further details. In the lower jaw, not only is the dentary elongated in concert with the occluding maxilla above it, but so is the supradentary/coronoid element (as would be expected, as it covers the alveoli medially), splenial, prearticular, and surangular, and likely the angular too. In particular, the surangular, although missing part of its middle portion, is clearly anteroposteriorly elongate and dorsoventrally shallow, as in *Alioramus altai* (Brusatte et al., 2012). Adult deep-snouted tyrannosaurids, on the other hand, have a shorter and deeper surangular (e.g., Carr, 1999, 2020; Hurum and Currie, 2000; Brochu, 2003; Currie, 2003; Hurum and Sabath, 2003; Loewen et al., 2013). Thus, both the front and back of the mandible are 'stretched' in alioramins despite the fact that the snout is elongated in the cranium, and not the temporal region (portion of the cranium posterior to the lacrimal). Additionally, the anterior palatal bones of alioramins (vomer and palatine) are clearly anteroposteriorly elongated compared with deep-snouted tyrannosaurids. The ectopterygoid, however, is not. Unfortunately, the fragmentary and broken nature of the pterygoid in known *Qianzhousaurus* and *Alioramus* specimens makes it difficult to compare the shape and proportions of this bone to deep-snouted tyrannosaurids.

Alioramin Ontogeny and Growth

In this section the specimens are treated as exemplars of growth stages, not taxa. In the absence of a growth series for

any single alioramin taxon, the objective is to recover a composite growth series based on the only available specimens. The data set consists of hypothetical growth characters that show an increase in relative development between specimens (Brinkman, 1988). It has been shown that some taxonomic characters are ontogenetically emergent (e.g., Carr, 2020) and so features of that type are included here since it cannot be known a priori which characters are not also growth informative.

Much of the variation seen between alioramins is consistent with growth trends seen in other tyrannosaurids (Table 1) (Carr, 1999, 2010, 2020; Carr and Williamson, 2004). Therefore, the three taxa (*Alioramus altai*, *Alioramus remotus*, *Qianzhousaurus sinensis*) are treated here as a proxy growth series, in order to assess the relative maturity of the type specimens and to make predictions about the growth series of each species, pending future discoveries of additional alioramin material. This section begins with a summary of the growth trends seen among alioramins and it ends with an assessment of the relative maturity of each type specimen.

Pneumatization—As in other tyrannosaurids (Carr, 1999, 2020), alioramins show a trend of increased pneumatization, including lengthening of the maxillary fenestra from short (*A. altai*) to long (*Q. sinensis*), maxillary pneumatic fossae that change from shallow (*A. altai*) to deep (*Q. sinensis*), and the cornual process of the lacrimal changing from non-inflated (*A. altai*) to inflated (*Q. sinensis*) (Table 1).

Tooth Count Reduction—Alioramins, like other tyrannosaurines (Carr, 1999, 2020; Carr et al., 2017), show a growth-related reduction in tooth count. The maxillary tooth count starts high, at 18 alveoli (*A. altai*), reduces to 16 (*A. remotus*), and finally to 15 (*Q. sinensis*). The shape of the alveoli (from 8-shaped to cartouche-shaped) reflect the transition from narrow ziphiform (*A. altai*) to wide incrassate teeth (*Q. sinensis*). The same trends are seen in the dentary, where the count starts at 20 alveoli (*A. altai*) and reduces to 18 (*A. remotus*, *Q. sinensis*), and the alveoli show the same shape differences as are seen in the maxilla that reflect the growth-related increase in tooth width. Note that we have elected to use the term 'ziphiform' to describe the discreet

TABLE 1. Assessment of the relative maturity of the holotype specimens of *Alioramus remotus* (PIN 3141/1), *A. altai* (IGM 100/1844), and *Qianzhousaurus sinensis* (GM F10004), assuming that these taxa share the same growth progression with other tyrannosaurids. If true, then the weight of evidence supports the hypothesis that the holotype of *Q. sinensis* is more mature than that of *A. altai*. Symbols: an asterisk (*) marks character transformation series not seen in other tyrannosaurids.

Bone	Character	*Alioramus altai*	*A. remotus*	*Qianzhousaurus sinensis*
Maxilla	promaxillary fenestra	not close to maxillary fenestra (0)	-	close to maxillary fenestra (1)
	accessory pneumatic fenestra	shallow fossa (0)	-	recess (1)
	subcutaneous surface, texture	smooth (0)	-	coarse (1)
	base of interfenestral strut	flat (0)	-	fossa present (1)
	tooth count	18 (0)	16 (1)	15 (2)
	teeth	ziphiform (0)	-	incrassate (1)
	alveoli, shape	pinched (0)	-	cartouche (1)
Nasals	lateral frontal process	short (0)	-	long (1)
	midline rugosities	small (0)	tall cusps (2)	large (1)
	caudal internasal suture	long (0)	-	short (1)
Lacrimal	lacrimal horn, size	small (0)	-	large (1)
	lacrimal horn, inflation	not inflated (0)	-	inflated (1)
Jugal	lateral cornual process	small & conical (0)	-	massive & indistinct (1)
	joint surface for the postorbital	shallow notch (0)	-	deep interlocking notch (1)
Postorbital bar	anteroposterior length	short (0)	-	long (1)
Postorbital	general form	gracile (0)	gracile (0)	stout (1)
	cornual process, form	subtle (0)	subtle (0)	large (1)
	cornual process, size	does not reach dorsal edge of bone (0)	does not reach dorsal edge of bone (0)	exceeds dorsal edge of bone (1)
	posterior process, form	curved (0)	curved (0)	straight (1)
	posterior process, length	long (0)	-	short (1)
	ventral ramus, process above jugal contact	absent (0)	present (1)	present (1)
	ventral ramus, orientation*	ventral (0)	-	anteroventral (1)
	subocular process, presence	absent (0)	present (1)	present (1)
Squamosal	ventral postorbital process, exposure	concealed (0)	exposed (1)	exposed (1)
	dorsal postorbital process, form	prominent (0)	gracile (1)	gracile (1)
	angle between postorbital and quadratojugal processes*	wide (0)	narrow (1)	narrow (1)
	laterotemporal fossa, depth*	subtle (0)	-	deep and distinct (1)
	posterior process, form	small (0)	-	large (1)
Dentary	ventral margin, form*	straight (0)	straight (0)	sinuous (1)
	subcutaneous surface, texture	smooth (0)	-	coarse (1)
	symphysis, texture	subtly coarse (0)	-	coarse (1)
	dental alveoli, number	20 (0)	18 (1)	18 (1)
	dental alveoli, shape	square, sharp-corners, 8-shaped (0)	-	rectangular, rounded corners (1)
Prearticular	shape	long and shallowly curved (0)	-	short, deeply curved (1)
Splenial	posterior notch, form*	small and acute (0)	-	large and obtuse (1)
	anterior mylohyoid foramen, form	long and shallow (0)	-	long and deep (1)
	anterior mylohyoid foramen, position*	close to ventral margin of bone (0)	-	far dorsal to ventral margin of bone (1)

dention of *A. altai*. We believe this descriptor to be of greater anatomical accuracy than the admittedly more widely used 'ziphodont.'

Ornamentation—Cephalic ornaments in alioramins show the same trends that are seen in other tyrannosaurids (Carr, 1999, 2020; Carr and Williamson, 2004), including increase in size of the midline bumps of the nasals that start small (*A. altai*), enlarge (*Q. sinensis*), and become tall cusps (*A. remotus*); increase in size of the cornual process of the lacrimal from small (*A. altai*) to large (*Q. sinensis*), which in part is enhanced by pneumatic inflation; and increase in the size of the cornual process of the postorbital from subtle (*A. altai*, *A. remotus*) to large, such that it exceeds the dorsal edge of the bone (*Q. sinensis*). One ornamental growth change is novel: the lateral rugose process of the jugal (which is absent from all other tyrannosaurids) starts small and conical (*A. altai*), becoming massive and indistinct (*Q. sinensis*).

Subcutaneous Surface—As in other tyrannosaurids (Carr, 2020), the subcutaneous surface of the maxilla and dentary of alioramins changes from smooth (*A. altai*) to coarse (*Q. sinensis*).

Joint Surfaces and Sutures—As in other tyrannosaurids (Brusatte and Carr, 2016; Carr, 2020), the joint surfaces and sutures of alioramins show growth-related changes. The posterior internasal suture changes from long (*A. altai*) to short (*Q. sinensis*), implying sequential ossification of the fibrous connective tissue that once separated the complements (Lü et al., 2014); the joint surface for the postorbital on the jugal changes from a shallow (*A. altai*) to a deep interlocking notch (*Q. sinensis*); and the symphysis of the dentary changes from subtly coarse (*A. altai*) to coarse (*Q. sinensis*). An increase in the length of a joint surface may result from a corresponding increase in the length of the process that bears it. For example, the lateral frontal process of the nasal changes from short in *A. altai* (relative to most other tyrannosaurids) to long in *Q. sinensis* (Fig. S1), the posterior process of the postorbital changes from curved and long (*A. altai*, *A. remotus*) to straight and short (*Q. sinensis*), and the stout process above the joint surface for the jugal of the postorbital is initially absent (*A. altai*) and later develops (*A. remotus*, *Q. sinensis*).

Skull Frame—Despite their low skulls, alioramins share many changes to the skull frame with other tyrannosaurids (Carr, 1999, 2020). The postorbital bone changes from gracile (*A. altai*, *A. remotus*) to stout (*Q. sinensis*). The postorbital bar changes from anteroposteriorly short (*A. altai*) to long (*Q. sinensis*). The subocular process of the postorbital changes from absent (*A. altai*) to present (*A. remotus*, *Q. sinensis*), reflecting the increase in height of the skull frame. The dorsal postorbital process of the squamosal changes from prominent (*A. altai*) to gracile (*A. remotus*, *Q. sinensis*).

Some skull frame changes to the cranium are novel: the orientation of the ventral process of the postorbital changes from vertical (*A. altai*) to anteroventral (*Q. sinensis*); the angle between the postorbital and quadratojugal processes of the squamosal changes from obtuse (*A. altai*) to acute (*A. remotus*, *Q. sinensis*), possibly reflecting the increased height of the skull frame; the ventral postorbital process of the squamosal changes from being concealed (*A. altai*) to exposed (*A. remotus*, *Q. sinensis*); and the posterior process of the squamosal changes from small (*A. altai*) to large (*Q. sinensis*).

As is seen in other tyrannosaurids (Carr, 1999, 2020; Carr and Williamson, 2004), the lower jaw increases in dorsoventral height, as indicated by several growth changes, including: the prearticular changes from long and shallowly curved (*A. altai*) to short and deeply curved (*Q. sinensis*); the posterior notch of the splenial changes from small and acute (*A. altai*) to large and obtuse (*Q. sinensis*); and the anterior mylohyoid foramen changes from long, shallow, and positioned close to the ventral edge of the bone (*A. altai*) to long, deep, and far dorsal to the ventral edge (*Q. sinensis*). One growth change is novel: the ventral margin of the dentary changes from straight (*A. altai*, *A. remotus*) to sinuous (*Q. sinensis*).

Muscle Scars and Fossae—The fossa between the postorbital and quadratojugal processes of the squamosal changes from subtle (*A. altai*) to deep and distinct (*Q. sinensis*), possibly indicating enhancement of the size and strength of the muscle. In other tyrannosaurids this fossa simultaneously increases in size but becomes shallow, not deep (Carr, 2020).

Quantitative Cladistic Analysis of Ontogeny—In order to objectively assess the relative maturity of the three holotypes, the data in Table 1 were converted into a matrix of 35 hypothetical growth characters (Appendix 1; Supplementary Data) in Mesquite v. 3.04 (Maddison and Maddison, 2019) and an artificial embryo was added to optimize the characters (see protocols in Carr, 2020; Appendix 2), and an exhaustive search of the character matrix was run in PAUP* v. 4.0a (Swofford, 2002).

A single ontogram was recovered (36 steps, CI 1.0), where the holotypes of *A. remotus* and *Q. sinensis* were recovered as more mature than *A. altai*. This growth series is consistent with the increase in skull length seen between the specimens, from smallest (*A. altai*; 63 cm; Lü et al., 2014) to largest (*Q. sinensis*; 90 cm). The level of maturity shared by *A. remotus* and *Q. sinensis* is supported by the unambiguous presence of six synontomorphies, including: in lateral view, a stout process from the postorbital that extends above the joint surface for the jugal, the presence of a subocular process on the ventral ramus of the postorbital, exposure of the ventral postorbital process of the squamosal, marginal exposure of the dorsal postorbital process of the squamosal in lateral view, an acute angle between the postorbital and quadratojugal processes of the squamosal, and a reduction in dentary tooth count.

Four characters show that the holotype of *Q. sinensis* is more mature than that of *A. remotus*, including: in lateral view, the stout form of the postorbital, the enlarged cornual process of the postorbital, the straight posterior process of the postorbital, and the sinuous ventral margin of the dentary. In contrast, *A. remotus* shares three relatively immature character states with *A. altai*, including: in lateral view, a gracile postorbital with a small cornual process and curved posterior process, and a straight ventral margin of the dentary.

This result at first glance appears to be at odds with the tall nasal cusps seen in *A. remotus*, but reduction in cephalic ornamentation is seen in other tyrannosaurids (Carr, 2020) and among ornithischian dinosaurs (e.g., Horner and Goodwin, 2008, 2009) and so alioramins show the ancestral dinosaurian pattern of growth-related ornament resorption. The presence of a subocular process in the mature specimens, and the curved prearticular in *Q. sinensis*, is evidence that the skull frame of alioramins do have a subtle growth-related increase in skull and jaw height, but not to the extreme that is seen in other tyrannosaurids.

Based on comparison with the growth series of *Tyrannosaurus rex* (Carr, 2020), *A. altai* corresponds to the juvenile growth stage (shallow skull frame, small cornual process of lacrimal and postorbital), *A. remotus* corresponds to young adults (increase in height of skull frame, reduced tooth count, enhanced nasal ornamentation), and *Q. sinensis* corresponds to relatively more mature adults (smooth nasals, maximally inflated cornual process of the lacrimal, large cornual process of the postorbital).

Since many of the differences between alioramins can be accounted for by growth, this winnows down the number of taxonomic differences between the three named species. Alioramin ontogeny is not marked by secondary metamorphosis and so niche partitioning between juveniles and adults was likely absent, in contrast to its presence in *T. rex* (Snively et al., 2019; Carr, 2020; Schroeder et al., 2021). Relative to the ancestral condition for tyrannosaurids, the enhanced snout length of alioramins is peramorphic (vs. short snout), whereas the low skull height is pedomorphic (vs. deep skull).

Based on the results found here, we make several predictions:

1. Histological aging of the three alioramin specimens will be congruent with the character-based growth series.
2. Growth series of multiple specimens of *A. altai*, *A. remotus*, and *Q. sinensis* that include juveniles, young adults, and adults will find the same sequence of character changes recovered in this proxy growth series.
3. Growth series of alioramins will clarify the changes to the skull and jaws of tyrannosaurids in general that are not dependent upon the increase in skull height.
4. The holotype of *Q. sinensis* represents the adult level of maturity and so represents the maximum ratio of skull height to skull length achieved by adult alioramins.
5. The apomorphic long-snouted condition will be seen in juvenile alioramins that are less mature than *A. altai*, including hatchlings; the developmental capture of derived adult skull shape is also seen in *T. rex* (Carr, 2020).
6. Histological evidence will show that the lifespan of alioramins is comparable to the plesiomorphic lifespan of other tyrannosaurids (e.g., 18–28 years; Erickson et al., 2004) and that the growth rate will be low as is seen in other tyrannosaurids aside from *T. rex* (27–33; Cullen et al., 2021), which has an apomorphically high growth rate.
7. Upon discovery of growth series for each species, the ontogenetic transition from ziphiform to incrassate maxillary and dentary teeth in alioramins will be found to correlate with a size-dependent increase in bite force.

Paleoecology of *Qianzhousaurus* and Alioramins

The largest derived tyrannosaurids such as *Tyrannosaurus* and *Tarbosaurus* used their tremendous bite strength and robust dentition (Erickson et al., 1996; Gignac and Erickson, 2017) to eat large prey such as ceratopsians and hadrosauroids (e.g., DePalma et al., 2013), and to break and swallow chunks of bone while doing so (Chin et al., 1998). This so-called 'puncture-pull' feeding would have given these species, or at least the most mature individuals among them, access to larger prey and a nutrition source (bone itself) that smaller and weaker-biting theropods could not exploit. In their description of *Alioramus altai*, Brusatte et al. (2009) hypothesized that its long-snouted, gracile skull lacked many of the cranial adaptations for puncture-pull feeding, such as a deep skull, robust bones, fused or highly interlocking sutures between various skull bones, a rugose and thickened lacrimal-postorbital bar above the orbit that could act as a stress sink (Henderson, 2003), a rigid lower jaw with a strongly interlocking dentary symphysis (Therrien et al., 2021), and thick incrassate teeth. Thus, they suggested that *Alioramus* exploited a different feeding style from the deep-snouted bone-biters, instead focusing on smaller prey. This may have been instrumental in allowing the contemporary *Alioramus* and *Tarbosaurus* to partition niches. Although Lü et al. (2014) did not discuss the feeding style of *Qianzhousaurus* in detail, they implied that it was similar to *Alioramus*, despite its larger size and somewhat more robust skull.

We here briefly discuss the biting and feeding style of *Qianzhousaurus*, as inferred from gross osteology of the skull. Three general observations suggest that *Qianzhousaurus*, unlike its deep-snouted cousins, would not have been a particularly hard biter. First, its teeth are intermediate between the mediolaterally thin ziphiform teeth of *Alioramus altai* and the robust, peg-like incrassate condition seen in adult derived tyrannosaurids. Second, although more robust than *Alioramus*, the skull bones of *Qianzhousaurus* are generally more gracile, with thinner rami and less reinforced sutures, than are those of deep-snouted tyrannosaurids (Rayfield, 2004, 2005a, b). Third, *Qianzhousaurus* possesses relatively smaller muscle attachment sites and evident muscle scarring relative to deep-skulled tyrannosaurid specimens (Hurum and Currie, 2000)—for instance, the flange for the adductor muscles above the surangular shelf and the muscle attachment site on the dorsal prong of the surangular anterior ramus are relatively smaller than those of deeper-snouted tyrannosarids. We thus predict that *Qianzhousaurus* would have filled a different ecological niche from large-bodied tyrannosaurids such as *Tarbosaurus*.

It is notable that alioramins existed in sympatry with deep-snouted tyrannosaurids. We envision that alioramins—both the smaller and more gracile *Alioramus* individuals and the moderately larger and more mature *Qianzhousaurus* holotype individual—would have been nimbler, perhaps more active pursuit predators than the hard-biting, but slower and stockier, apex predators such as *Tarbosaurus*. Recent research into tyrannosaurid-dominated ecosystems finds that the diversity of large-bodied theropods in these faunas is remarkably low, which is likely due to ontogenetically controlled niche partitioning within single species, with juvenile tyrannosaurids filling niches traditionally occupied by separate taxa of small–medium sized theropods in non-tyrannosaurid-dominated environments (Woodward et al., 2020; Garcia-Giron et al., 2021; Holtz, 2021; Schroeder et al., 2021). This does raise a key question about the ecology of alioramins: were *Alioramus* and *Qianzhousaurus* also competing with the juveniles of their deep-skulled cousins? If so, how was this possible? Were there other anatomical, behavioral, or environmental factors that helped them partition niches? It also remains mysterious why there were separate taxa of long-snouted tyrannosaurids (alioramins) in Asia at the very end of the Cretaceous, but not in the even better-sampled North America.

We here propose some hypotheses, which can be tested with future study. We suggest that the long and delicate snout of alioramins effectively barred them from killing the same prey as both juveniles and subadults of *Tarbosaurus bataar*. We hypothesize there was little dietary competition between the lineages, although subadult and adult *Ta. bataar* could have preyed upon the smaller and relatively defenseless (aside from speed) alioramins. The specialized alioramin snout and dentition prevented competitive overlap, in terms of diet, between the sympatric lineages. Likewise, juvenile and subadult *Ta. bataar* of the same size as alioramins had higher bite forces that prevented or modulated competition since they could capably attack large prey that alioramins could not kill. In terms of Asian tyrannosaurine evolution, we propose that the slender alioramin skull was in a novel gracile lane (there is no analog of alioramins in the Laramidia or Appalachia subdivisions of North America in the Cretaceous), perhaps limited to killing small animals, whereas the boxy skull of *Ta. bataar* stayed in the ancestral lane of killing large animals. In contrast to the situation in Laramidia, where competition for similar prey could not have been avoided between *Gorgosaurus libratus* and *Daspletosaurus torosus* (given their similar morphotypes; cf. Russell, 1970), alioramins evolved specializations that, beyond preventing competition with *Ta. bataar*, secured their place in Upper Cretaceous Asian terrestrial ecosystems, presumably all the way up to the K/Pg extinction event.

We note that what is outlined above is at the hypothesis stage. Our prediction that *Qianzhousaurus* (and *Alioramus*) were weaker biters not capable of puncture-pull feeding needs to be tested explicitly using biomechanical analysis, such as Finite Element Analysis like that performed for other tyrannosaurids (Rayfield et al., 2001; Meers, 2003; Rayfield, 2004; Rayfield, 2005a, b; Rowe and Snively, 2021). Such analyses will be the best judge of the bite force estimates and structural integrity of the longirostrine alioramin skull, and how they compare with deep-snouted tyrannosaurids, and what that implies about dietary differences and niche partitioning. In addition to the

discovery of even more mature (e.g., fully adult) alioramin specimens, such biomechanical analyses will be the next step in understanding the growth, feeding, and paleobiology of the unusual, long-snouted tyrannosaurids that lived at the same time as their deep-snouted kin, at the very end of the Age of Dinosaurs.

ACKNOWLEDGMENTS

Funding was provided by Natural Science Foundation of China grants (41272022) to J. L., NSF GRF, DDIG (DEB 1110357), the American Museum of Natural History Division of Paleontology, and Columbia University to S. L. Brusatte. S. L. Brusatte thanks his good friend, the late J. Lü for many years of collaboration and camaraderie, and his friends at the Ganzhou Museum for their hospitality and support during his research visit to study *Qianzhousaurus* with J. Lü in 2014. We thank F. Ma and W. Xuefang for assistance and discussion. We also thank J. Voris and our other reviewers for their insight and assistance.

ORCID

William Foster http://orcid.org/0000-0002-7398-2143
Stephen L. Brusatte http://orcid.org/0000-0001-7525-7319
Thomas D. Carr http://orcid.org/0000-0001-9000-0132
Thomas E. Williamson http://orcid.org/0000-0002-2856-9632

LITERATURE CITED

Bever, G. S., S. L. Brusatte, A. M. Balanoff, M. A. Norell. 2011. Variation, variability, and the origin of the avian endocranium: insights from the anatomy of Alioramus altai (Theropoda: Tyrannosauroidea). PLoS One 9 8:23393.

Bever, G. S., S. L. Brusatte, T. D. Carr, X. Xu, A. M. Balanoff, and M. A. Norell. 2013. The Braincase Anatomy of the Late Cretaceous dinosaur Alioramus (Theropoda: Tyrannosauroidea). Bulletin of the American Museum of Natural History 376:1–72.

Brinkman, D. 1988. Size-independant criteria for estimating relative age of *Ophiacodon* and *Dimetrodon* (Reptillia, Pelycosauria) from the Admiral and lower Belle Plains formations of west-central Texas. Journal of Vertebrate Paleontology 2: 172–180.

Brochu, C. A. 2003. Osteology of *Tyrannosaurus rex*: insights from a nearly complete skeleton and high-resolution computed tomographic analysis of the skull. Journal of Vertebrate Palaeontology 22(sup4):1–138.

Brusatte, S. L and T. D. Carr. 2016. The phylogeny and evolutionary history of tyrannosauroiddinosaurs. Scientific Reports 6:1–8.

Brusatte, S. L., R. B. Benson, and M. A. Norell. 2011. The anatomy of *Dryptosaurus aquilunguis* (Dinosauria: Theropoda) and a review of its tyrannosauroid affinities. American Museum Novitiates 3717:1–53.

Brusatte, S. L., T. D. Carr, and M. A. Norell. 2012. The osteology of *Alioramus*, a gracile and long-snouted tyrannosaurid (Dinosauria: Theropoda) from the Late Cretaceous of Mongolia. Bulletin of the American Museum of Natural History 366:1–197.

Brusatte, S. L., G. T. Lloyd, S. C. Wang, M. A. Norell. 2014. Gradual assembly of avian body plan culminated in rapid rates of evolution across the dinosaur-bird transition. Current Biology. 24(10):2386–2392.

Brusatte, S. L., T. D. Carr, G. M. Erickson, G. S. Bever, and M. A. Norell. 2009. A long-snouted, multihorned tyrannosaurid from the Late Cretaceous of Mongolia. Proceedings of the National Academy of Sciences. 106(41):17261–17266.

Brusatte, S. L., M. A. Norell, T. D. Carr. G. M. Erickson, J. R. Hutchinson, A. M. Balanoff, G. S. Bever, J. N. Choiniere, P. J. Makovicky, and X. Xu. 2010. Tyrannosaur Palaeobiology: new research on ancient exemplar organisms. Science. 329(5998):1481–1485.

Carr, T. D. 1999. Craniofacial ontogeny in tyrannosauridae (Dinosauria, Coelurosauria). Journal of Vertebrate Paleontology 19(3):497–520.

Carr, T. D. 2010. A taxonomic assessment of the type series of *Albertosaurus sarcophagus* and the identity of Tyrannosauridae (Dinosauria, Coelurosauria) in the Albertosaurus bonebed from the Horseshoe Canyon Formation (Campanian-Maastrichtian, Late Cretaceous). Canadian Journal of Earth Sciences 47:1213–1226.

Carr, T. D. 2020. A high-resolution growth series of *Tyrannosaurus rex* obtained from multiple lines of evidence. PeerJ 8:e9192.

Carr, T. D., and T. E. Williamson. 2004. Diversity of Late Maastrichtian Tyrannosauridae (Dinosauria: Theropoda) from western North America. Zoological Journal of the Linnean Society 142(4):479–523.

Carr, T. D., and T. E. Williamson. 2010. *Bistahieversor sealeyi*, gen. et sp. Nov., a new tyrannosauroid from New Mexico and the origin of deep snouts in Tyrannosauroidea. Journal of Vertebrate Palaeontology 30(1):1–16.

Carr, T. D., T. E. Williamson, and D. R. Schwimmer. 2005. A new genus and species of tyrannosauroid from the Late Cretaceous (Middle Campanian) Demopolis Formation of Alabama. Journal of Vertebrate Paleontology 25(1):119–143.

Carr, T. D., D. J. Varracchio, J. C. Sedlmayr, E. M. Roberts, and J. R. Moore. 2017. A new tyrannosaur with evidence for anagenesis and crocodile-like facial system. Scientific Reports 7:44942.

Chin, K., T. T. Tokaryk, G. M. Erickson, and L. C. Calk. 1998. A king-sized theropod coprolite. Nature 393(6686):680–682.

Cullen, T. M., L. Zanno, D. W. Larson, E. Todd, P. J. Currie, and D. C. Evans. 2021. Anatomical, morphometric, and stratigraphic analyses of theropod biodiversity in the Upper Cretaceous (Campanian) Dinosaur Park Formation. Canadian Journal of Earth Sciences 58 (9): 870–884.

Currie, P. J. 2003. Cranial anatomy of tyrannosaurid dinosaurs from the Late-Cretaceous of Alberta, Canada. Acta Palaeontologica Polonica 48(2).

Currie, P. J., and D. Zhiming. 2001. New information on Cretaceous troodontids (Dinosauria, Theropoda) from the People's Republic of China. Canadian Journal of Earth Sciences 38(12):1753–1766.

DePalma, R. A., D. A. Burnham, L. D. Martin, B. M. Rothschild, and P. L Larson. 2013. Physical evidence of predatory behaviour in *Tyrannosaurus rex*. Proceedings of the National Academy of Sciences 110(31):12560–12564.

Erickson, G. M., P. J. Makovicky, P. J. Currie, and M. A. Norell. 2004. Gigantism and comparative life-history parameters of tyrannosaurid dinosaurs. Nature 430: 772–775.

Erickson, G. M., S. D. Van Kirk, J. Su, M. E. Levenston, W. E. Caler, and D. R. Carter. 1996. Bite-force estimation for *Tyrannosaurus rex* from tooth-marked bones. Nature 382(6593):706–708.

Garcia-Giron, J., J. Heino, J. Alahuhta, A. A. Chiarenza, and S. L. Brusatte. 2021. Palaeontology meets metacommunity ecology: the Maastrichtian dinosaur fossil record of North America as a case study. Palaeontology 64(3):335–357.

Gauthier, J. 1986. Saurichian monophyly and the origin of birds. Memoirs of the California Academy of Sciences 8:1–55.

Gignac, P. M., and G. M. Erickson. 2017. The biomechanics behind extreme osteophagy in *Tyrannosaurus rex*. Scientific Reports 7(1):1–10.

Gold, M. E. L., S. L. Brusatte, and M. A. Norell. 2013. The cranial pneumatic sinuses of the tyrannosaurid *Alioramus* (Dinosauria: Theropoda) and the evolution of cranial pneumaticity in theropod dinosaurs. American Museum Novitiates 3790:1–46.

Henderson, D. M. 2003. The eyes have it: the sizes, shapes, and orientations of theropod orbits as indicators of skull strength and bite force. Journal of Vertebrate Paleontology 22(4):766–778.

Holtz Jr, T. R. 2001. The phylogeny and taxonomy of the Tyrannosauridae. Mesozoic Vertebrate Life 64–83.

Holtz Jr, T. R. 2021. Theropod guild structure and the tyrannosaurid niche assimilation hypothesis: implications for predatory dinosaur macroecology and ontogeny in later Late Cretaceous Asiamerica. Canadian Journal of Earth Sciences, 99(999):1–18.

Hone, D. H., K. Wang, C. Sullivan, X. Zhao, S. Chen, D. Li, S. Ji, Q. Ji, and X. Xu. 2011. A new, large tyrannosaurine theropod from the Upper Cretaceous of China. Cretaceous Research 32(4):495–503.

Horner, J. R., and M. B. Goodwin. 2008. Ontogeny of cranial epi-ossifications in Triceratops. Journal of Vertebrate Paleontology 28(1):134–144.

Horner, J. R., and M. B. Goodwin. 2009. Extreme cranial ontogeny in the Upper Cretaceous dinosaur *Pachycephalosaurus*. PLoS ONE 4(10).

Hurum, J. R. H., and P. J Currie. 2000. The crushing bite of tyrannosaurids. Journal of Vertebrate Palaeontology 20(3):619–621.

Hurum, J. H., and K. Sabath. 2003. Giant theropod dinosaurs from Asia and North America: skulls of *Tarbosaurus bataar* and

Tyrannosaurus rex compared. Acta Palaeontologica Polonica 48 (2):161–190.
Hutt, S., D. Naish, D. M. Martill, M. J. Barker, and P. Newberry. 2001. A preliminary account of a new tyrannosauroid theropod from the Wessex Formation (Early Cretaceous) of southern England. Cretaceous Research 22(2):227–242.
Kurzanov, S. M. 1976. A new Late Cretaceous carnosaur from the Nogon-Tsav, Mongolia. Sovmestnaâ Sovetsko-Mongolskaâ Paleontologiceskaâ Ekspeditciâ Trudy 3:93–104.
Lambe, L. M. 1917. The Cretaceous theropodus dinosaur *Gorgosaurus*. Memoirs of the Geological Survey of Canada 100:1–84.
Loewen, M. A., R. B. Irmis, J. J. Sertich, P. J. Currie, and S. D. Sampson. 2013. Tyrant dinosaur evolution tracks the rise and fall of Late Cretaceous oceans. PLoS One 8(11)e79420.
Lü, J., L. Yi, S. L. Brusatte, L. Yang, H. Li, and L. Chen. 2014. A new clade of Asian Late Cretaceous long-snouted tyrannosaurids. Nature Communications 5(3788).
Maddison, W. P. and D. R. Maddison. 2019. Mesquite: a modular system for evolutionary analysis. Version 3. 61. Http://www.mesquieproject.org
Maleev, E. A. 1974. Giant carnosaurs of the family Tyrannosauridae. The joint Soviet-Mongolian Paleontological Expedition transactions 1:132–191.
Marsh, O. C. 1881. Principal characters of American Jurassic dinosaurs, part V. American Journal of Science, 3(125): 417–423.
Meers, M. B. 2003. Maximum bite force and prey size of *Tyrannosaurus rex* and their relationships to the inference of feeding behaviour. Historical Biology 16(1):1–12.
Molnar, R. E. 1991. The cranial morphology of *Tyrannosaurus rex*. Palaeontographica. Abteilung A, Paläozoologie, Stratigraphie 217:137–176.
Olshevsky, G. 1995. The origin and evolution of the tyrannosaurids. Kyoryugaku Saizensen 9:92–119.
Osborn, H. F. 1905. Tyrannosaurus and other Cretaceous carnivorous dinosaurs. Bulletin of the AMNH 21(14).
Osborn, H. F. 1912. Crania of *Tyrannosaurus* and *Allosaurus*. Memoirs of the American Museum of Natural History 1:33–54.
Owen, R. 1842. Report on British Fossil Reptiles. Part II. Reports of the British Association for the Advancement of Science, 11:60–204.
Parks, W. A. 1928. *Albertosaurus arctunguis*: a new species of therapodus dinosaur from the Edmonton Formation of Alberta. University of Toronto Studies Geological Series 26:1–24.
Rauhut, O. W., A. C. Milner, and S. Moore-Fay. 2010. Cranial osteology and phylogenetic position of the theropod dinosaur *Proceratosaurus bradleyi* (Woodward, 1910) from the Middle Jurassic of England. Zoological Journal of the Linnean Society 158(1):155–195.
Rayfield, E. J. 2004. Cranial mechanics and feeding in *Tyrannosaurus rex*. Proceedings of the Royal Society of London Series B: Biological Sciences 271(1547):1451–1459.
Rayfield, E. J. 2005a. Using finite-element analysis to investigate suture morphology: a case study using large carnivorous dinosaurs. The Anatomical Record Part A: Discoveries in Molecular, Cellular, and Evolutionary Biology: An Official Publication of the American Association of Anatomists 283(2):349–365.
Rayfield, E. J. 2005b. Aspects of comparative cranial mechanics in the theropod dinosaurs *Coelophysis*, *Allosaurus* and *Tyrannosaurus*. Zoological Journal of the Linnean Society 144(3):309–316.
Rayfield, E. J., D. B. Norman, C. C. Horner, P. M. Smith, J. J. Thomason, and P. Upchurch, 2001. Cranial design and function in a large theropod dinosaur. Nature 409(6823):1033–1037.
Rowe, A. J., and E. Snively. 2021. Biomechanics of juvenile tyrannosaurid mandibles and their implications for bite force. The Anatomical Record early view.
Russell, D. A. 1970. Tyrannosaurs from the Late Cretaceous of Western Canada. National Museum of Natural Sciences Publications in Paleontology 1:1–34.
Schroeder, K., S. K. Lyons, F. A. Smith, 2021. The influence of juvenile dinosaurs on community structure and diversity. Science 371 (6532):941–944.
Sereno, P. C., L. Tan, S. L, Brusatte, H. J. Kriegstein, X. Zhao, and K. Cloward. 2009. Tyrannosaurid skeletal design first evolved at small body size. Science 326(5951):418–422.
Snively, E. H., D. M. Henderson, and D. S. Phillips. 2006. Fused and Vaulted nasals of tyrannosaurir dinosaurs: implications for cranial strength and feeding mechanics. Acta Palaeontologica polonica 51(3).
Snively, E. H., D. M. O'Brien, M. Henderson, H. Mallison, L. Surring, M. E. Burns, T. R. Holtz Jr, A. P. Russel, L. M. Witmer, P. J. Currie, S. A. Hartman, and J. R. Cotton. 2019. Lower rotational intertia and larger leg muscles indicate more rapid turns in tyrannosaurids than in other large theropods. PeerJ 7:e6432.
Swofford, D. L. 2002. PAUP*, Phylogenetic Analysis Using Parsimony (*and other methods). Version 4. Sinauer Associated, Sunderland, Massachusetts.
Therrien, F., D. K. Zelenitsky, J. T. Voris, and K. Tanaka. 2021. Mandibular force profiles and tooth morphology in growth series of *Albertosaurus sarcophagus* and *Gorgosaurus libratus* (Tyrannosauridae: Albertosaurinae) provide evidence for an ontogenetic dietary shift in tyrannosaurids. Canadian Journal of Earth Sciences Just-IN. p.52
Tsuihiji, T., M. Watabe., K. Tsogtbaatar., K. Tsubamoto., T. Barsbold., R. Suzuki., S. Lee., A. H. Ridgely., Y. Kawahara, and L. M. Witmer. 2011. Cranial osteology of a juvenile specimen of *Tarbosaurus bataar* (Theropoda, Tyrannosauridae) from the Nemegt Formation (Upper Cretaceous) of Bugin Tsav, Mongolia. Journal of Vertebrate Paleontology. 31(3):497–517.
Von Huene, F. 1914. Das natürliche system der Saurischia. Zentralblatt Mineralogie, Geologie, und Palaeontologie B:154–158.
Witmer, L. M. 1997. The evolution of the antorbital cavity of archosaurs: a study in soft-tissue reconstruction in the fossil record with an analysis of the function of pneumaticity. Journal of Vertebrate Paleontology 17(1):1–76.
Woodward, H. N., K. Tremaine, S. A. Williams, L. E. Zanno, J. R. Horner, and N. Myhrvold. 2020. Growing up *Tyrannosaurus rex*: Osteohistology refutes the pygmy "*Nanotyrannus*" and supports ontogenetic niche partitioning in juvenile *Tyrannosaurus*. Science Advances 6(1):p. eaax6250.
Xu, X., M. A. Norell, X. Kuang, X. Wang, Q. Zhao, and C. Jia. 2004. Basal tyrannosauroids from China and evidence for protofeathers in tyrannosauroids. Nature 431(7009):680.
Xu, X., J. M. Clark, C. A. Forster, M. A. Norell, G. M. Erickson, D. A. Eberth, C. Jia, and Q. Zhao. 2006. A basal tyrannosauroid dinosaur from the Late Jurassic of China. Nature 439(7077):715.
Xu, X., K. Wang, K. Zhang, Q. Ma, L. Xing, C. Sullivan, D. Hu, S. Cheng, and S. Wang. 2012. A gigantic feathered dinosaur from the Lower Cretaceous of China. Nature 484(7392):92–95.

Submitted May 4, 2021; revisions received September 27, 2021;
accepted October 18, 2021.
Handling Editor: Amy Balanoff.

APPENDIX 1. Character list used to resolve the proxy alioramin growth series based on data from the holotypes of *Alioramus altai* (IGM 100/1844), *A. remotus* (GIN 3141/1), and *Qianzhousaurus sinensis* (GM F10004).

1. **Maxilla, promaxillary fenestra, proximity to maxillary fenestra, lateral view**: not close (0), close (1).
2. **Maxilla, accessory pneumatic fenestra, depth of invasion, lateral view**: shallow (0), recess (1).
3. **Maxilla, subcutaneous surface, texture, lateral view**: smooth (0), coarse (1).
4. **Maxilla, interfenestral strut, base, form, lateral view**: flat (0), concave (1).
5. **Maxilla, tooth count**: 18 (0), 16 (1), 15 (2).
6. **Maxilla, dental alveoli, shape, ventral view**: 8-shaped (0), cartouche (1).
7. **Nasal, lateral frontal process, length, dorsal view**: short, where in dorsal view the processes are only slightly longer than the medial frontal processes (0); long, where in dorsal view the lateral processes are separated by a deep wedge of the frontal and they are twice as long as the medial frontal process (1). See Supplemental Data for an imaged clarification of both states of this character.
8. **Nasal, midline rugosities, size, lateral view**: small (0), large (1), tall cusps (2).

9. **Nasal, caudal internasal suture, length, dorsal view**: long (0), short (1).
10. **Lacrimal, cornual process, size, lateral view**: small (0), large (1).
11. **Lacrimal, cornual process, inflation, lateral and dorsal views**: not inflated (0), inflated (1).
12. **Jugal, lateral cornual process, size, lateral view**: small (0), massive (1).
13. **Jugal, postorbital suture, lateral view**: shallow notch (0), interlocking (1).
14. **Postorbital bar, anteroposterior length, lateral view**: narrow (0), wide (1).
15. **Postorbital, form, lateral view**: gracile (0), stout (1).
16. **Postorbital, cornual process, form, lateral view**: small (0), large and exceeds dorsal margin of bone (1).
17. **Postorbital, posterior process, form, lateral view**: curved (0), straight (1).
18. **Postorbital, posterior process, length, lateral view**: long and reaches posterior end of laterotemporal fenestra (0), short and stops short of the end of the fenestra (1).
19. **Postorbital, ventral ramus, process above joint surface for the jugal, presence, lateral view**: absent (0), present (1).
20. **Postorbital, ventral ramus, orientation, lateral view**: ventral (0), anteroventral (1).
21. **Postorbital, subocular process, presence, lateral view**: absent (0), present (1).
22. **Squamosal, ventral postorbital process, exposure, lateral view**: concealed (0), exposed (1).
23. **Squamosal, dorsal postorbital process, exposure, lateral view**: prominent (0), reduced (1).
24. **Squamosal, angle between postorbital and quadratojugal processes, lateral view**: wide (0), narrow (1).
25. **Squamosal, laterotemporal fossa, depth, lateral view**: shallow (0), deep (1).
26. **Squamosal, posterior process, size, lateral view**: small (0), large (1).
27. **Dentary, ventral margin, form, lateral view**: straight (0), sinuous (1).
28. **Dentary, subcutaneous surface, texture, lateral view**: smooth (0), coarse (1).
29. **Dentary, symphysis, texture, medial view**: subtly coarse (0), coarse (1).
30. **Dentary, tooth count**: 20 (0), 18 (1).
31. **Dentary, dental alveoli, shape, dorsal view**: eight-shaped (0), cartouche-shaped (1).
32. **Prearticular, shape, lateral and medial views**: long and shallow (0), deep and curved (1).
33. **Splenial, posterior notch, form, lateral and medial views**: small and acute (0), large and obtuse (1).
34. **Splenial, anterior mylohyoid foramen, lateral and medial views**: shallow (0), deep (1).
35. **Splenial, anterior mylohyoid foramen, dorsoventral position relative to the ventral edge of the bone, lateral and medial views**: close to ventral margin (0), far dorsal to ventral margin (1).

APPENDIX 2. The character matrix used to resolve the proxy alioramin growth series based on data from the holotypes of *Alioramus altai* (IGM 100/1844), *A. remotus* (GIN 3141/1), and *Qianzhousaurus sinensis* (GM F10004).

	1	2	3	
Taxon	1234567890	1234567890	1234567890	12345
Artificial embryo	0000000000	0000000000	0000000000	00000
Alioramus altai	0000000000	0000000000	0000000000	00000
A. remotus	????1???2?	????000?1?	1111??0??1	?????
Qianzhousaurus sinensis	1111211111	1111111111	1111011111	11111